SOVIET PHYSICS USPEKHI VOLUME 9, NUMBER 6 MAY-JUNE 1967

621.373.1

GAS LASER IN A MAGNETIC FIELD

M. I. D'YAKONOV and S. A. FRIDRIKHOV

A. F. Ioffe Physico-technical Institute, Academy of Sciences, U.S.S.R.; Leningrad Polytechnic Institute

Usp. Fiz. Nauk 90, 565–600 (December, 1966)

CONTENTS

DURING the five years elapsed since the construction of the first gas laser by Javan, Bennet, and Herriot [1], a tremendous number of papers have been published devoted to the investigation of different physical processes connected with generation of light by an active gas medium. In particular, extensive material has been accumulated on the influence of magnetic fields on the operation of the gas laser. A study of this question is important both for a better understanding of the laser electrodynamics and for practical purposes (tuning and stabilization of the frequency, increase of laser power, etc.). The behavior of a gas laser in a magnetic field therefore becomes of increasing interest both to experimenters and to theoreticians. Sufficiently detailed theoretical studies in this field were made, however, only quite recently, following the publication of the well known paper by Lamb [2]. A number of effects observed when a gas laser is placed in a magnetic field are now qualitatively understood, but more detailed experimental and theoretical work in this field is needed. The purpose of the present review is to detail the main features of the behavior of a gas laser in a magnetic field and to systematize the published data on this question.

I. MAGNETOOPTICAL EFFECTS IN A GAS LASER

1. Introductory Remarks

A magnetic field can influence the operation of a gas laser in two ways. First, the magnetic field causes Zeeman splitting of the working levels of the gas atoms. This splitting gives rise to a number of magnetooptic effects, consisting in changes of the intensity, generation frequencies, and polarization of the laser emission. Second, a sufficiently strong magnetic field in a gas-discharge laser can influence the gas-discharge plasma characteristics (the electron density and the temperature), which determine the pumping rates at the upper and lower levels. Changes in the intensity of gas-discharge laser emission resulting from the influence of the magnetic field on the pumping will henceforth be called arbitrarily "plasma-optic effects." These effects usually become noticeable at magnetic field intensities on the order of several hundred Oersted.

Most studies of magnetooptic effects in gas lasers were made in He-Ne lasers. Principal attention was paid to the influence of the magnetic field on generation at wavelengths 0.63, 1.15, and 3.39 μ. In Paschen's notation, these wavelengths correspond to the transitions $3s_2 - 2p_4$, $2s_2 - 2p_4$, and $3s_2 - 3p_4$ of the neon atom. The upper working levels for these transitions have a total angular momentum $j_1 = 1$, and the lower ones have $j_0 = 2$. The experimental values of the g-factors for these levels are [3] 1.295, 1.184, and 1.301 for the $3s_2$, $3p_4$, and $2p_4$ levels, respectively. Fork and Patel [4] obtained $g = 1.33$ for the $2s_2$ level. Calculation of the g-factors by the $[jl]$-coupling scheme [5] gives a value $g = 4/3$ for all these levels.

It is well known that an atomic level characterized by a total angular-momentum quantum number j splits in a magnetic field $\mathbf{H}$ into $2j + 1$ sublevels having different magnetic quantum numbers. The energy spacing between two neighboring sublevels is $g\mu_0 H$, where μ_0 is the Bohr magneton. The selection rules for the dipole radiation allow only those transitions between the sublevels of the upper and lower states, at which the magnetic quantum number does not change (π-components), or changes by ± 1 (σ^+ and σ^- components). The Zeeman splitting of the levels

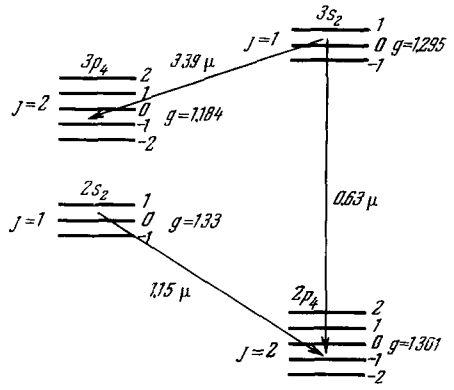

FIG 1 Zeeman splitting of the levels $3s_2$, $3p_4$, $2s_2$, and $2p_4$ of the neon atom

$3s_2$, $3p_4$, $2s_2$, and $2p_4$ of the neon atom is shown in Fig. 1.

The gas intensification (absorption) line has in the absence of a magnetic field, as is well known, a Doppler contour with center at the transition frequency ω_0 and with width determined by the transition wavelength and by the thermal velocity of the atoms. (For example, for the $\lambda = 1.15\ \mu$ Ne line at room temperature the Doppler width is ~ 800 MHz).

In a magnetic field, the intensification line generally splits into several components. In particular, in a longitudinal magnetic field, the Doppler contour for the transition $j_1 = 1 \rightarrow j_0 = 2$ splits into six components three of which intensify the light with right-hand circular polarization (RCP), and three with left-hand circular polarization (LCP). If the g-factors of the upper and lower states are the same, then the Zeeman splitting for these states are equal, and the intensification line in the longitudinal field splits only into two components corresponding to the intensification of the light with RCP and LCP. For the fundamental lines of the He-Ne laser, the g-factors of the upper and lower working levels differ little from each other. In a weak magnetic field, this difference can be neglected. In strong fields, however, the difference in the g-factors can become significant (see Sec. 6).

Magnetooptic effects in a gas laser are the consequence of the splitting of the intensification line of the active medium in a magnetic field. This splitting, for example, complicates the effect of frequency pulling and leads to the occurrence of low-frequency beats in the laser emission (see Sec. 4). In addition, an important role can be played by nonlinear effects connected with the motion of the dips on the intensification line when the magnetic field changes.

We confine ourselves in this review to the operation of a laser in a constant and homogeneous magnetic field*. We assume also that the Zeeman splitting is much smaller than the splitting due to the fine structure. The magnetooptic effects are dealt with in Secs. 2—5. These effects are usually observed at magnetic fields such that the change in the plasma parameters under the influence of the magnetic field can be neglected. In Secs. 6 and 7 we touch upon questions of practical utilization of magnetooptic effects. An analysis of plasma-optic effects is given in Secs. 8 and 9. We shall use circular frequencies in our formulas, but the values of the oscillation frequencies and of the frequency intervals will be given in Hz.

*Culshaw and Kannelaud[6] obtained in their experiments interesting data on the influence of an alternating magnetic field on the emission of a gas laser This question, however, has been little studied and calls for further investigation

2. Fundamentals of the Theory of a Gas Laser in a Magnetic Field

Laser theory is based on simultaneous solution of Maxwell's equations for the electrodynamic field in a resonator and the material equations describing the behavior of the active medium.

The theory of the gas laser was developed by Lamb[2]. He started from the assumptions that the working levels are not degenerate and that the laser emission is linearly polarized in a definite direction (the latter assumption is justified for a laser with Brewster windows). The magnetooptic effects in a gas laser are connected with the splitting of the working levels in a magnetic field, and therefore the theory of such effects must take into account the real Zeeman structure of the levels. In a laser without a preferred polarization direction (which we shall henceforth denote as "flat" for brevity) the emission polarization depends significantly on the magnetic field and cannot be regarded as fixed.

We present below the fundamentals of the theory of a gas laser in the presence of a magnetic field (see[7-12]).

We confine ourselves to the single-mode regime. Then the electric field in the laser can be represented by

$$\mathcal{E}(s, t) \quad [\mathbf{e}(t) + \mathbf{e}^*(t)] \sin ks, \tag{2.1}$$

where $k = n\pi/L$, n is an integer, L is the distance between mirrors, and s is the coordinate along the laser axis. As usual, we neglect the weak dependence of the field on the transverse coordinates. The field (2.1) induces a dipole moment in the gas. We denote the positive frequency contribution to the density of this dipole moment by $\mathcal{P}(s, t)$. From Maxwell's equations we can obtain the following equation for $e(t)^2$:

$$\frac{d^2\mathbf{e}}{dt^2} + \frac{\omega_n}{Q}\frac{d\mathbf{e}}{dt} + \omega_n^2\mathbf{e} = -4\pi\frac{d^2\mathbf{P}}{dt^2}, \tag{2.2}$$

where

$$\mathbf{P}(t) = \frac{2}{L}\int_0^L \mathcal{P}(s, t)\sin ks\, ds \tag{2.3}$$

is that part of the dipole moment $\mathcal{P}(s, t)$ which has the same spatial distribution as the field $\mathcal{E}$, $\omega_n = kc$

is the natural frequency of the resonator for the mode in question, and Q is the resonator figure of merit.

The problem thus consists of finding the quantity $\mathbf{P}(t)$ with account of the fact that the gas is in a magnetic field. An important factor in this case is that the induced dipole moment is connected with the radiation field in nonlinear fashion, since the radiation influences the polarizability of the active medium. To investigate the main effects which arise when the gas laser is placed in a magnetic field, it is sufficient following Lamb's procedure [2], to calculate the dipole moment $\mathbf{P}$ accurate to terms of third order in the electric field intensity in the resonator. Such calculations were made by a number of workers. Fork and Sargent [7] and Rozanov and Tulub [9] calculated the polarizability of the gas in a longitudinal magnetic field for the simplest case when the total angular momenta of the upper (j_1) and lower (j_0) working levels were equal to unity and zero, respectively. The value of $\mathbf{P}$ for arbitrary angular momenta j_1 and j_0 in the case of a longitudinal magnetic field was calculated in [8]. An expression suitable for quantitative calculations of the nonlinear polarizability of the gas at arbitrary values of j_1 and j_0 and at arbitrary direction of the magnetic field was derived in a paper by Perel' and one of the authors [12], where account was also taken of the spontaneous transition from the upper to the lower level.

Let the upper and lower working levels be characterized by total angular momenta of the atom j_1 and j_0 by g-factors g_1 and g_0, and by lifetimes γ_1^{-1} and γ_0^{-1}, respectively. We shall number the Zeeman sublevels of the upper state by the symbols m and m′, and the sublevels of the lower state by μ and μ'. The state of the active medium is described by the density matrix $\hat{f}$, which depends on the coordinate s, the projection of the atom velocity along the resonator axis v, and the time t. The matrix elements of $\hat{f}$ pertaining to the upper and lower state will be denoted by $f_{mm'}$ and $f_{\mu\mu'}$, respectively. The elements of the density matrix relating the upper and lower states will be denoted by $f_{\mu m}$ and $f_{m\mu} = f^*_{\mu m}$. The equations of motion in the presence of a magnetic field H are

$$\frac{\partial f_{mm'}}{\partial t} + v\frac{\partial f_{mm'}}{\partial s} = (-\gamma_1 - i\Omega_{mm'})f_{mm'} + \frac{i}{\hbar}\sum_{\mu}[(\mathcal{E}\mathbf{d}_{m\mu})f_{\mu m'} - f_{m\mu}(\mathcal{E}\mathbf{d}_{\mu m'})] + \gamma_1 N_1 F(v)\delta_{mm'},$$

$$\frac{\partial f_{\mu\mu'}}{\partial t} + v\frac{\partial f_{\mu\mu'}}{\partial s} = (-\gamma_0 - i\Omega_{\mu\mu'})f_{\mu\mu'} + \frac{i}{\hbar}\sum_{m}[(\mathcal{E}\mathbf{d}_{\mu m})f_{m\mu'} - f_{\mu m}(\mathcal{E}\mathbf{d}_{m\mu'})] + \gamma_0 N_0 F(v)\delta_{\mu\mu'},$$

$$\frac{\partial f_{\mu m}}{\partial t} - v\frac{\partial f_{\mu m}}{\partial s} = (-\gamma_{10} - i\Omega_{m\mu} + i\omega_0)f_{\mu m} + \frac{i}{\hbar}\left[\sum_{m_1}(\mathcal{E}\mathbf{d}_{m_1 m})f_{m_1 m} - \sum_{\mu_1} f_{\mu\mu_1}(\mathcal{E}\mathbf{d}_{\mu_1 m})\right]. \quad (2.4)$$

Here $\mathbf{d}_{m\mu}$ is the matrix element of the atomic dipole-moment operator, $\Omega_{mm'} = (m - m')\Omega_1$, $\Omega_{\mu\mu'} = (\mu - \mu')\Omega_0$, $\Omega_{\mu m} = \mu\Omega_0 - m\Omega_1$, $\hbar\Omega_1 = \mu_0 g_1 H$, $\hbar\Omega_0 = \mu_0 g_0 H$, μ_0 is the Bohr magneton, $\gamma_{10} = (\gamma_1 + \gamma_0)/2$, and $\delta_{mm'}$ and $\delta_{\mu\mu'}$ are Kronecker symbols. N_1 has the meaning of the population of an individual Zeeman sublevel of the upper state, which would be produced by the pumping in the absence of an emission field in the laser, and N_0 is the same for the lower state. It is assumed that the pumping is homogeneous and isotropic, and that the atoms in the upper and lower levels are produced with Maxwellian velocity distributions. F(v) is the Maxwellian distribution normalized to unity. The quantization axis is chosen to coincide with the direction of the magnetic field H (z axis).

After solving (2.4) it is necessary to calculate the density of the dipole moment $\mathcal{P}(s, t)$ which enters in (2.3), using the formula

$$\mathcal{P}(s, t) = \int_{-\infty}^{\infty} dv \sum_{m\mu} f_{\mu m}(s, v, t)\,\mathbf{d}_{m\mu}. \quad (2.5)$$

Equations (2.1)—(2.5) constitute a complete system describing the behavior of a gas laser operating in the single-mode regime in a magnetic field. The expression obtained in the general case [12] for $\mathbf{P}$ is quite cumbersome. We present formulas derived for a longitudinal magnetic field under the assumption that the g-factors of the upper and lower levels are equal* (this assumption is well justified for the fundamental lines of the He-Ne laser). Then $\Omega_1 = \Omega_0 = \Omega$. The calculation of the dipole moment $\mathbf{P}$, accurate to terms cubic in the electric field, yields [11, 12]

$$P_q = \chi_q e_q, \quad (2.6)$$

where P_q and e_q ($q = \pm 1$) are the circular components of the vectors $\mathbf{P}$ and e respectively: $P_1 = -(P_x + iP_y)/\sqrt{2}$, $P_{-1} = (P_x - iP_y)/\sqrt{2}$. The z axis coincides with the s axis. The nonlinear polarizability χ_q (with $\gamma_{10} \ll ku$) is given by the expressions

$$\chi_1 = a_1 - b_{11}|e_1|^2 - b_{1,-1}|e_{-1}|^2,$$
$$\chi_{-1} = a_{-1} - b_{-1,1}|e_1|^2 - b_{-1,-1}|e_{-1}|^2, \quad (2.7)$$

where

$$a_q = \alpha e^{-\xi_q^2}\left(i + \frac{2}{\sqrt{\pi}}\int_0^{\xi_q} e^{t^2}\,dt\right), \quad (2.8)$$

$$b_{11} = i\frac{3}{4}\frac{|d|^2}{\hbar^2\gamma_{10}}\alpha e^{-\xi_q^2}\cdot 1_1\left(\frac{1}{\gamma_1} + \frac{1}{\gamma_0}\right)\left[1 - \frac{\gamma_{10}}{\gamma_{10} + i(\delta - \Omega)}\right],$$

$$b_{1,-1} = i\frac{3}{4}\frac{|d|^2}{\hbar^2\gamma_{10}}\alpha e^{-\xi_q^2}\left\{\left(\frac{A_2}{\gamma_0} + \frac{A_3}{\gamma_1}\right)\left(\frac{\gamma_{10}}{\gamma_{10} - i\Omega} - \frac{\gamma_{10}}{\gamma_{10} + i\delta}\right) - \left(\frac{A_2}{\gamma_1 - 2i\Omega} + \frac{A_3}{\gamma_0 - 2i\Omega}\right)\left(\frac{\gamma_{10}}{\gamma_{10} - i\Omega} + \frac{\gamma_{10}}{\gamma_{10} + i(\delta - \Omega)}\right)\right\},$$

$$b_{-q,-q'}(\Omega) = b_{q,q'}(-\Omega). \quad (2.9)$$

*An expression for the polarizability χ_q when $g_1 \neq g_0$ is given in [8].

Here $\alpha = \pi^{1/2}|d|^2(N_1 - N_0)/3\hbar ku$, $\xi_q = (\delta - q\Omega)/ku$, $\delta = \omega_n - \omega_0$ is the resonator detuning, d is the reduced matrix element of the dipole moment, and u is the most probable velocity of the atom. The numbers A_1, A_2, and A_3 depend only on the values of j_1 and j_0, and are expressed in terms of 6j-symbols. When $j_1 = 1$ and $j_0 = 2$ we have $A_1 = 23/450$, $A_2 = 1/900$, and $A_3 = 7/300$. A criterion for the applicability of the method of successive approximations, with the aid of which formulas (2.6)—(2.9) were obtained, is the condition $|e_q d|^2 \ll \hbar^2\gamma_1\gamma_0$.

Let us discuss the foregoing results. a_q is the usual linear polarizability of the gas in the magnetic field. Its imaginary part (when $N_1 > N_0$) is the gain at the generation threshold, and the real part determines the dispersion. The imaginary part $a''_\pm$ has as a function of the magnetic field a maximum at $\Omega = \pm\delta$ and drops off at the Doppler line width, when $\xi_\pm \sim 1$. The quantity ku is connected with the width $\Delta\omega_D$ of the Doppler contour at half the height by the relation $\Delta\omega_D = 2\sqrt{\ln 2}\,ku$.

The second and third terms in (2.7) describe the nonlinear influence of the laser radiation on the polarizability of the active medium. We see that the polarizability χ_1 for the RCP radiation, with account of the nonlinearity, is altered not only by the field e_1 but also by the field e_{-1}. Let us examine the influences of the "own" and "foreign" fields separately. The electric field in the laser is a standing wave (2.1) which can be represented as a superposition of two waves traveling in the positive and negative directions. Therefore the right-polarized radiation is amplified by atoms with velocities satisfying the condition

$$\omega_n = \omega_0 + \Omega \pm kv, \qquad (2.10)$$

and this equality could be satisfied accurate to the quantity γ_{10}. It is known that the radiation tends to equalize the populations at the levels between which the transition is effected. Therefore the field e_1 decreases the inverse population for the two groups of atoms with velocities $v \approx \pm(\delta - \Omega)/k$ and thus decreases the gain $\chi''_1 = \mathrm{Im}\,\chi_1$. From condition (2.10) we see that when $\Omega = \delta$ the wave e_1, which travels in both the positive and negative directions, reduces the inverse population for the same atoms with velocities $v \approx 0$. Therefore when $\delta = \Omega$ the field e_1 will have the largest nonlinear influence on the polarizability χ_1. In accord with the foregoing, the diagonal coefficient b_{11} in (2.7) has, in agreement with (2.9), a resonant singularity at $\Omega = \delta$. At a specified intensity $I_1 = |e_1|^2$, the gain for the right-polarized radiation should decrease sharply at $\Omega = \delta$. Actually, however, during the generation the gain remains at all time equal to the loss, and therefore in order to maintain the gain at the specified level the intensity I_1 should decrease at $\Omega = \delta$.

The "foreign" field e_{-1} decreases the population inversion for atoms with velocities such that

$$\omega_n = \omega_0 - \Omega \pm kv. \qquad (2.11)$$

(The ± sign again corresponds to waves traveling in the positive and negative directions.) From a comparison of the conditions (2.11) and (2.10) we see that when $\Omega = 0$ the same atoms amplify the right-polarized radiation e_1. An identical situation obtains when $\omega_n = \omega_0 (\delta = 0)$. Then the atoms whose inverse population is reduced by the LCP wave, traveling in the positive direction participate in the amplification of the RCP wave traveling in the negative direction, and vice-versa. It is seen from (2.9) that the nondiagonal coefficients $b_{1,-1}$ and $b_{-1,1}$ actually have resonant singularities at $\Omega = 0$ and at $\delta = 0$. The second term in the curly brackets in expression (2.9) for the nondiagonal coefficient $b_{1,-1}$ is connected with the existence of nondiagonal elements in the density matrixes $f_{mm'}$ and $f_{\mu\mu'}$ ("coherence"). When $\Omega \gg \gamma_1, \gamma_0$ this term becomes negligible.

The physical cause of the interaction of the fields with RCP and with LCP is that the σ^+ and σ^- transitions can begin (or terminate) at the same Zeeman sublevels. There exists, however, a special case, not yet realized in practice ($j_1 = j_0 = 1/2$), when this is not so. Calculation [12] shows that in this case the nondiagonal elements are equal to zero, i.e., the fields of different polarizations do not influence each other. The influence of the field of one polarization on the polarizability for the other is also due to spontaneous transition from the upper working level to the lower one [12]. However, if the probability of such a transition is small compared with the probability of transitions to all remaining levels, then this influence can be neglected. For the case of a longitudinal magnetic field, let us substitute (2.6) in (2.2) and put $e_1(t) = E_1 \exp(i\omega_1 t)$ and $e_{-1}(t) = E_{-1}\exp(i\omega_{-1}t)$. Then, neglecting as usual the small terms, we obtain

$$\left(\frac{i}{Q} - \frac{2\Delta_1}{\omega_n}\right) E_1 = 4\pi\chi_1 E_1, \quad \left(\frac{i}{Q} - \frac{2\Delta_{-1}}{\omega_n}\right) E_{-1} = 4\pi\chi_{-1}E_{-1}, \qquad (2.12)$$

where $\Delta_1 = \omega_1 - \omega_n$ and $\Delta_{-1} = \omega_{-1} - \omega_n$ are the shifts of the generation frequencies for the right and left polarizations. Equations (2.12) and (2.7) allow us to determine the intensities $I_1 = |e_1|^2$ and $I_{-1} = |e_{-1}|^2$ and the frequency shifts Δ_1 and Δ_{-1} for a flat laser in the stationary regime.

In a laser with Brewster windows, the emission remains linearly polarized if the pumping is not too large. We take the x axis to be the polarization direction. Then $e_1 = -e_{-1} = -e_x/\sqrt{2}$. Using (2.6) and putting $e_x = E\exp(i\omega_x t)$, we obtain for this case

$$\frac{i}{Q} - \frac{2\Delta_x}{\omega_n} = \frac{1}{2}(4\pi\chi_1 + 4\pi\chi_{-1}), \qquad \Delta_x = \omega_x - \omega_n, \qquad (2.13)$$

where we now must put $I_1 = I_{-1} = I/2$ in expression (2.7) for χ_q.

For a transverse magnetic field it is easy to obtain equations similar to (2.12) and (2.13) [12]. Equations of type (2.12) are nonlinear algebraic equations

and have in general several solutions. It is therefore necessary to ascertain which of the solutions is stable and is realized in practice. The stability of different types of oscillations was investigated in [12]:

3. Influence of Magnetic Field on the Intensity

A weak magnetic field greatly influences the intensity of the gas-laser emission.

It follows from (2.12) and (2.7) that for a flat laser in a longitudinal magnetic field it is possible to have either only left-polarized or only right-polarized emission, or else both waves exist simultaneously. An analysis shows [12] that at not too large a detuning and not too strong magnetic fields, the stable regime is one in which both polarizations, E_1 and E_{-1}, coexist. In this case, cancelling E_1 and E_{-1} from the equations of (2.12) and separating the imaginary part ($\chi_q = \chi'_q + i\chi''_q$), we get

$$4\pi\chi_1 = 1/Q, \quad 4\pi\chi'_{-1} = 1/Q. \tag{3.1}$$

The equations in (3.1) are simply the generation condition: the gain for each of the polarizations is equal to the loss. Before we present formulas for the emission intensity, let us attempt to obtain the main qualitative results without derivations. We introduce, following Bennet [13], the auxiliary quantity $\chi_q(\omega_c)$. This quantity has the meaning of polarizability for a weak signal of frequency ω_c propagating in a medium in which the velocity distribution of the excited atoms is distorted by a strong field of frequency ω_n. It is obvious that

$$\chi_q(\omega_c)|_{\omega_c=\omega_n} = \chi_q, \tag{3.2}$$

where the nonlinear polarizability χ_q is given by (2.7). A strong field reduces the inverse population for certain groups of atoms, leading to formation of dips in the gain for a weak signal $4\pi\chi''_q(\omega_c)$ [13]. For the two-level scheme usually employed in an analysis of a gas laser in the absence of a magnetic field, the following statement holds true: The intensity of the laser emission is proportional to the total area of the dips in the weak-signal gain. When the Zeeman splitting in a magnetic field is taken into account, this statement is in general incorrect. We can, however, consider a simplified model [11], in which it holds true in this case, too. This model is based on the assumption that the density matrices of the upper and lower states can be written in the form $f_{mm'} = \delta_{mm'} f_1$ and $f_{\mu\mu'} = \delta_{\mu\mu'} f_0$, i.e., the populations of all the Zeeman sublevels are equal and there is no "coherence" between the different Zeeman sublevels.* In addition, as above, we assume that the g-factors of the working levels are equal. The simplified model describes correctly the main features of the phenomena in question, and permits their simple physical interpretation. We shall henceforth follow the exposition in [11]. We shall show first how the concept of dips explains the well known effect that in the absence of a magnetic field the radiation intensity decreases at exact tuning of the cavity [2,14]. Figure 2a shows (for $\Omega = 0$) the quantity $4\pi\chi''_{-1}(\omega_c)$ against the weak-signal frequency ω_c. The width of the entire curve is determined by the Doppler line width ku. The curve has two dips, one at $\omega_c = \omega_n$ and the other is symmetrical to it relative to the center of the line ω_0. The generation condition (3.1) requires that the bottom of each dip be tangent to the horizontal line $4\pi\chi''_q(\omega_c) = 1/Q$. The widths of the dips are determined by the half-sum of the natural widths of the working levels γ_{10}. When the resonator is tuned to the center of the atomic line ($\omega_n = \omega_0$) the dips coalesce (Fig. 2b). Compared with Fig. 2a, we see that the area of the dips, and consequently the radiation intensity, decreases in this case.

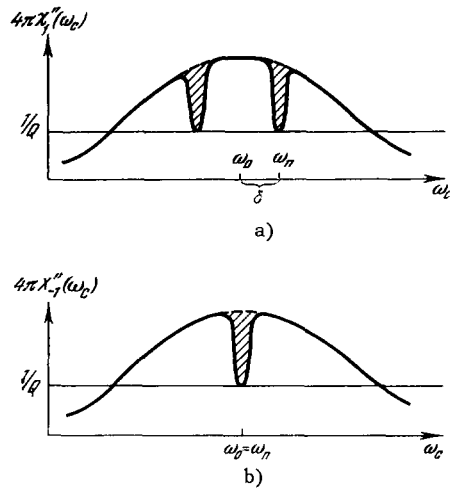

FIG. 2. Gain ($4\pi\chi''$) vs. weak-signal frequency ω_c in the presence of generation at frequency ω_n a) Resonator detuning $\delta = \omega_n - \omega_0 \neq 0$. b) $\delta = 0$ (resonator tuned to center of the atomic line).

Plots of the gains for right- and left-polarized weak signals $4\pi\chi''_{\pm1}(\omega_c)$ in the presence of a longitudinal magnetic field are shown in Fig. 3. The maxima of these curves are now shifted by an amount 2Ω (we recall that Ω is the distance between the Zeeman sublevels, which is assumed to be the same for the upper and lower states). Let us examine the plot of $4\pi\chi''_1(\omega_c)$. This curve shows four dips. The singly-shaped dips are connected with the distortion of the velocity distribution of the atoms under the influence of the strong field E_1 ("own" dips). The doubly-shaded dips are connected with the influence of the field E_{-1} ("foreign" dips). As already mentioned in Sec. 2, the fields E_1 and E_{-1} decrease the population inversion for the atoms whose velocity satisfies the conditions $\omega_n = \omega_0 + \Omega \pm kv$ and $\omega_n = \omega_0 - \Omega \pm kv$ respectively. These atoms participate in the intensification of the weak signal with RCP and

*This assumption can become justified to some degree if depolarizing collisions with small changes in velocity play a significant role

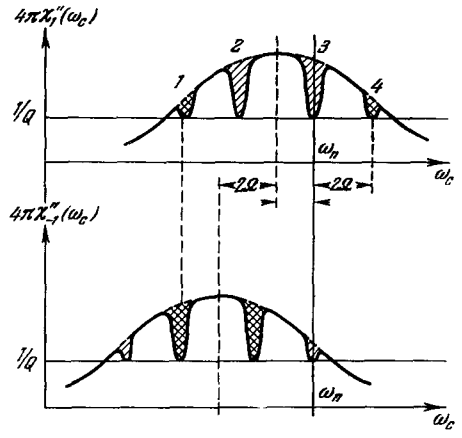

FIG. 3. Gains $4\pi\chi''_{\pm 1}$ for right- and left-polarized signal vs. signal frequency ω_c in the presence of a longitudinal magnetic field (Ω – distance between Zeeman sublevels; unmarked arrows indicate the region $\delta - \Omega$).

with frequency $\omega_c = \omega_0 + \Omega + kv$. Thus, the curve for $4\pi\chi''_1(\omega_c)$ acquires "own" dips at $\omega_c = \omega_n$ and $\omega_c = \omega_0 - \delta + 2\Omega$ and "foreign" dips at $\omega_c = \omega_0 + \delta + 2\Omega$ and $\omega_c = \omega_0 - \delta$. The dips on the $4\pi\chi''_{-1}(\omega_c)$ curve arise in similar fashion. In the simplified model considered by us, the dips caused by the field E_{-1} on the $4\pi\chi''_1(\omega_c)$ curve should be exactly the same as on the $4\pi\chi''_{-1}(\omega_c)$ curve.

As seen from Fig. 3, when the magnetic field tends to zero ($\Omega \to 0$), pairwise coalescence of the dips 1 with 2 and 3 with 4 takes place. Therefore the emission intensity decreases. Another singularity appears when the Zeeman splitting becomes equal to the cavity detuning. When $\Omega = \delta$, the "own" dips 2 and 3 coalesce, and the emission intensity again decreases. Physically, the decrease in the emission intensity upon coalescence of the dips is connected with the decrease in the number of atoms participating in the generation of the emission. Figure 4 (curve 1) shows schematically the dependence of the emission intensity on the applied longitudinal magnetic field. The intensity minimum at $\Omega = \delta$, connected with the coalescence of the "own" dips, has not been observed experimentally in so far as we know.

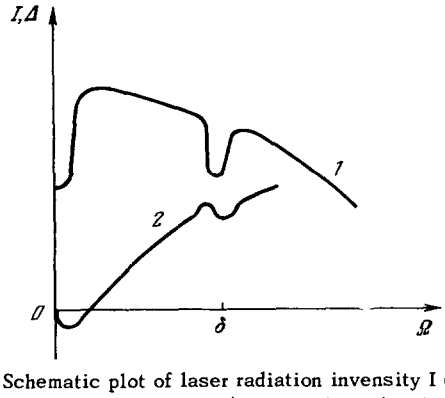

FIG. 4. Schematic plot of laser radiation invensity I (curve 1) and low-frequency beat frequency Δ (curve 2) vs. longitudinal magnetic field.

From (3.1) and (2.7)—(2.9) we can obtain the following formulas for the emission intensity of a flat laser:

$$I_1 = |e_1|^2 = D_1/D, \quad I_{-1} = |e_{-1}|^2 = D_{-1}/D, \tag{3.3}$$

$$D_1 = b''_{-1,-1}\left(a''_1 - \frac{1}{4\pi Q}\right) - b''_{1,-1}\left(a''_{-1} - \frac{1}{4\pi Q}\right),$$

$$D_{-1} = b''_{11}\left(a''_{-1} - \frac{1}{4\pi Q}\right) - b''_{-1,1}\left(a''_1 - \frac{1}{4\pi Q}\right),$$

$$D = b''_{11}b''_{-1,-1} - b''_{1,-1}b''_{-1,1}. \tag{3.4}$$

Here a″ and b″ denote the imaginary parts of the coefficients a and b, given by formulas (2.8) and (2.9). The dependence of the emission intensity on the longitudinal magnetic field for a laser with Brewster windows has the same singularity as in a flat laser. In this case we must use in lieu of (3.1) the condition $(4\pi\chi''_1 + 4\pi\chi''_{-1})/2 = 1/Q$. From this we obtain with the aid of (2.7)—(2.9) (where $I_1 = I_{-1} = 1/2$) the following expression for the emission intensity:

$$I = 2\frac{a''_1 + a''_{-1} - (2\pi Q)^{-1}}{b''_{11} + b''_{1,-1} + b''_{-1,1} + b''_{-1,-1}}. \tag{3.5}$$

From this formula and from expressions (2.8) and (2.9) for the coefficients a and b we see clearly the character of the $I(\Omega)$ dependence described above. Thus, the use of the simplified model, which presupposes a mixing of the population among the Zeeman sublevels, gives a correct qualitative description of the dependence of the intensity on the applied magnetic field. However, the influence of the nondiagonal elements $f_{mm'}$ and $f_{\mu\mu'}$ is not small, especially in weak magnetic fields, when the Hanle effect is superimposed on the phenomena discussed here and connected with the coalescence of the dips. In particular, a second minimum with a width determined by the smaller of the quantities γ_1 or γ_0, can become superimposed at $\Omega = 0$ on the intensity minimum of width γ_{10} (which is likewise at $\Omega = 0$).

In the presence of a transverse magnetic field, let us direct the y axis along the cavity axis s (the z axis is directed along the magnetic field). In this case the intensities I_x and I_z for a flat laser are determined from the equations

$$4\pi\chi''_x = 1/Q, \quad 4\pi\chi''_z = 1/Q,$$

where $\chi_x = (\chi_1 + \chi_{-1})/2$ and $\chi_z = \chi_0$. An analysis of the dips on the $\chi''_x(\omega_c)$ and $\chi''_z(\omega_c)$ curves shows that in addition to the singularities at $\Omega = 0$ and $\Omega = \delta$, a minimum of the intensity can arise at $\Omega = 2\delta$[11]. This minimum is connected with the coalescence of the "own" and "foreign" dips and therefore appears only if light of both polarizations is present in the laser emission.

The published experimental data on the influence of a weak magnetic field on the emission intensity of a gas laser pertain unfortunately only to the multimode regime. The lasers used in all such experi-

ments had Brewster windows. Apparently the first experiment of this type was carried out by Bunser et al.[15], who investigated the generation of an He-Ne laser at 1.15-μ wavelength in a longitudinal magnetic field. The pumping was with a high-frequency generator. They observed a weakly pronounced increase of intensity with increasing magnetic field from 0 to ~15 Oe. With further increase of the magnetic field, the emission intensity decreased monotonically, generation shutting off at H ~ 200 Oe. An increase in the pump shifted the shutoff point towards larger magnetic fields.

Similar results were obtained in the case of a longitudinal magnetic field at $\lambda = 1.15\ \mu$ by Culshaw and Kannelaud[16] and by Fotiadi and Fridrikhov[17]. Culshaw and Kannelaud used an He-Ne laser with a confocal-type cavity and excited with a high-frequency generator. The dependence they obtained for the intensity on the solenoid current (1 A = 40 Oe) is shown in Fig. 5. The upper curve corresponds to a larger pump power. The laser parameters are not given in[16].

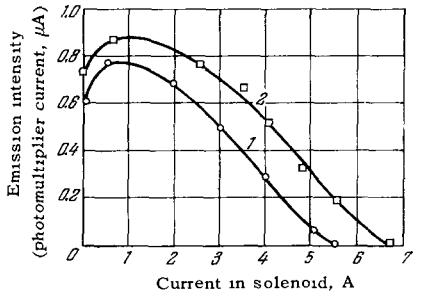

FIG. 5. Intensity of He-Ne laser emission ($\lambda = 1.15\ \mu$) vs. current in the solenoid (1 A = 40 Oe) at different pump powers [16]. (Curve 2 corresponds to a larger high-frequency pump power.)

In[17], a semi-confocal cavity was used with external dielectric mirrors, with a tube 1 m long and 8 mm in dia, and with Brewster-angle windows. The tube was placed along the axis of a solenoid of 70 cm length. The emission was registered with an FÉU-22 photomultiplier placed in the exit slit of an IKS-12 monochromator. Pumping with either high-frequency current or with dc was possible. Figure 6 shows the experimental data for the case of dc excitation. A small increase in intensity (by 8—15%) is observed in the region $0 < H < 15$ Oe, followed by a rather gently sloping maximum and a slow decrease. As seen from Fig. 6, at sufficiently large pump power, a plateau appears on the curves. With weak pumping, and also with high-frequency excitation, curves similar to those obtained in[15,16] are observed.

We make the following remarks concerning these experiments. A direct quantitative comparison of the results of these investigations with the theoretical

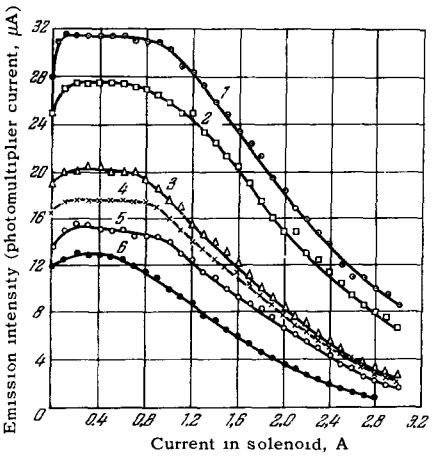

FIG. 6. Intensity of He-Ne laser emission ($\lambda = 1.15\ \mu$) vs. current in solenoid (1 A = 145 Oe) at different pump powers [17]. DC excitation with current I_p: 1 — 70 mA, 2 — 50 mA, 3 — 30 mA, 4 — 25 mA, 5 — 20 mA, 6 — 15 mA, p = 1 Torr, $p_{Ne}/p_{He} = 1/10$, tube diameter d = 6 mm.

calculations[7-12] pertaining to the single-mode regime is impossible. It is clear, however, that the intensity minimum at H = 0 has the same nature as in the single-mode regime. The Zeeman splitting Ω corresponding to the width of this minimum is ~20—40 MHz, which is in qualitative agreement with the published data[14] on the value of the γ_{10} for the $2s_2 - 2p_4$ transition of the Ne atom. The slow decrease in intensity when $\Omega > \gamma_{10}$ is connected with the decrease in the region of overlap of the gain curves for the transitions σ^+ and σ^-, and is similar to the decrease occurring, in accord with (3.5), in the single-mode regime.

We note that in the presence of a magnetic field in multimode operation, each mode corresponds in general to four dips in the gain $\chi_q''(\omega_c)$ for a weak signal. When the magnetic field is varied, the relative position of the dips changes. Coalescence of some dips should lead to a decrease in the emission intensity when a corresponding magnetic field intensity is reached. The picture is made more complicated by mode-competition effects. In addition, as shown by Javan and Szoke[18], the use of a natural isotope mixture does not make it possible to observe clearly the Lamb dip[2,14] which occurs in the absence of a magnetic field when the cavity is tuned exactly.

A similar appreciable smearing can occur, for example, in the minimum of the emission intensity at $\Omega = \delta$. (However, the minimum at $\Omega = 0$ does not become smeared.)

Terekhin and Fridrikhov[19] observed a minimum of intensity at H = 0 in the case of a longitudinal magnetic field for the red line $\lambda = 63\ \mu$. Figure 7 shows a series of curves plotted at a mixture pressure 0.85 Torr, which is close to optimal for the given tube diameter (4.5 mm). Unlike the curves of Fig. 6 for $\lambda = 1.15\ \mu$, in this case an appreciable

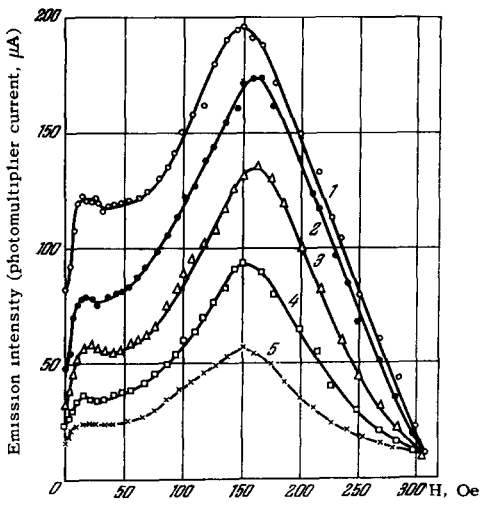

FIG. 7. Emission intensity of He-Ne laser ($\lambda = 63\ \mu$) vs. intensity of longitudinal magnetic field at different pump powers [19]. DC pumping. 1 – $I_p = 30$ mA, 2 – 40 mA, 3 – 50 mA, 4 – 60 mA, 5 – 70 mA, p = 0.85 Torr, $p_{Ne}/p_{He} = 1/5.6$, d = 4.5 mm

growth of emission intensity is observed in fields from 50 to 150 Oe. This growth is connected with the appearance of a competing transition at the wavelength $\lambda = 3.39\ \mu$, characterized by an exceedingly high gain. The width of the Doppler contour for the $\lambda = 3.39\ \mu$ (300 MHz) is much smaller than the corresponding width for $\lambda = 0.63\ \mu$ (1500 MHz). Therefore a magnetic field of ~100 Oe greatly reduces the gain for $\lambda = 3.39\ \mu$, leading to an increase in the population of the common upper level $3s_2$, and by the same token to an increase in the emission intensity of the red line.

This effect was first observed by Bell and Bloom[20]. Suppressing the emission at 3.39 μ, they succeeded in observing not only the growth of the emission intensity at 0.63 μ, but also generation at all the allowed transitions $3s_2 - 2p$. To separate the individual lines, a prism was placed in the resonator.

4. Beats in a Magnetic Field

An interesting effect occurring when a gas laser is placed in a magnetic field is the appearance of low-frequency beats between oscillations of different polarization[22]. These beats are the result of frequency pulling. It is known[13,14] that if the natural frequency ω_n of the cavity does not coincide with the atomic frequency, then the generation frequency shifts away from ω_n to the center of the atomic line. The shift is proportional in the linear approximation to the cavity detuning and to the ratio of the pass band of the cavity $\Delta\omega_n = \omega_n/Q$ to the width $\Delta\omega_D$ of the atomic line.

In a longitudinal magnetic field, the maxima of the gains for right- and left-polarization are shifted by an amount 2Ω. The frequencies of the oscillations with RCP and LCP are each attracted towards the center of its own line. Therefore for a flat laser the frequencies ω_1 and ω_{-1} become different, and beats with frequency $\omega_1 - \omega_{-1}$ can be observed in the emerging beam with the aid of a polarizer.

In a flat laser, when both polarizations E_1 and E_{-1} are present in the emission, the frequency shift is determined by the real part of the polarizability, using Eqs. (2.12)

$$\frac{2\Delta_1}{\omega_n} = -4\pi\chi_1', \quad \frac{2\Delta_{-1}}{\omega_n} = -4\pi\chi_{-1}', \tag{4.1}$$

where the intensities I_1 and I_{-1}, obtained from the conditions (3.1), should be substituted in formula (2.7) for χ_q'.

The nonlinear influence of the emission on the polarizability of the active medium, leading to the appearance of intensity minima (see Sec. 3), is also manifest in the dependence of the frequency shifts on the magnetic field[7-12,21]. It is convenient to investigate this dependence by analyzing the real part of the polarizability for a weak signal $\chi_q'(\omega_c)$.

The presence of a dip in the gain curve $4\pi\chi_1''(\omega_c)$ at a certain frequency corresponds to a nonmonotonic dispersion of $4\pi\chi_1''(\omega_c)$ near the same frequency (Fig. 8). The length of the segment AB on Fig. 8 is proportional, in accord with the first equation of (4.1) and condition (3.2), to the shift Δ_1 of the generation frequency. When dips 3 and 4 of Fig. 3 coalesce, the kink 4 in the dispersion curve in Fig. 8 runs into the point B, and this leads to a nonmonotonic dependence of the shift Δ_1 on the magnetic field. Such a nonmonotonicity will take place at $\Omega = 0$ and $\Omega = \delta$, i.e., in the same places where the emission intensity has minima. We note that this nonmonotonicity appears in fact at sufficiently strong pumping, which increases with increasing ratio γ_{10}/ku. Figure 4 shows schematically the dependence of the beat frequency $\Delta = \omega_1 - \omega_{-1} = \Delta_1 - \Delta_{-1}$ on the magnetic field at sufficiently large pumping (curve 2). We present a formula describing the dependence of the beat frequency Δ on the applied longitudinal magnetic field at exact tuning of the resonator[8]

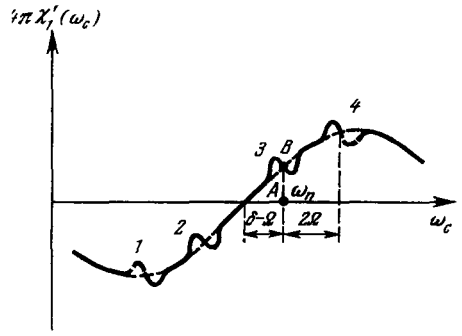

FIG. 8 Dispersion curve for a weak signal with RCP propagating in a gas medium and in the presence of generation at frequency ω_n. Longitudinal magnetic field (The kinks 1 – 4 correspond to the dips 1 – 4 on Fig 3.)

$$\Delta = -4\pi\omega_n \left[a_1' - \frac{b_{11}' + b_{1,-1}'}{b_{11}'' + b_{1,-1}''} \left(a_1'' - \frac{1}{4\pi Q} \right) \right]. \quad (4.2)$$

The coefficients a and b are given by formulas (2.8) and (2.9), where we must put in this case $\delta = 0$.

Figure 9 shows schematically a plot of $\Delta(\Omega)$ at different values of the pump energy in the region where $\Omega \ll ku$. Curves 1—7 are numbered in increasing order of pump energy. The straight line 1 corresponds to the generation threshold. With this,

$$a_1'' \approx \alpha = \frac{1}{4\pi Q}, \quad a_1' = -\alpha \frac{2}{\sqrt{\pi}} \frac{\Omega}{ku}$$

and

$$\Delta = \frac{2}{\sqrt{\pi}} \frac{\omega_n}{Q} \frac{\Omega}{ku}. \quad (4.3)$$

As the pump increases from threshold, the second term in formula (4.2) can become larger than the first, and Δ reverses sign. On the other hand, when $\Omega \gg \gamma_{10}$, the second term tends to zero, and the frequency Δ again becomes positive.

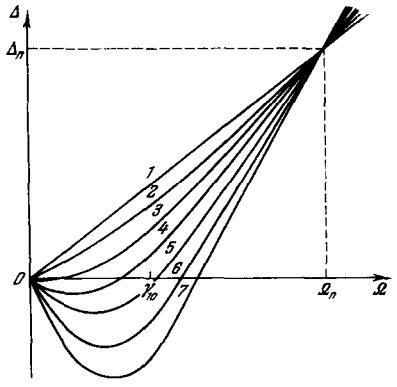

FIG. 9. Schematic plot of the beat frequency vs. the longitudinal magnetic field at exact resonator tuning ($\delta = 0$). (The pump increases from curve towards curve 7.)

As noted by Rozanov and Tulub [9], all curves should cross at the single point at $\Omega \sim (ku\gamma_{10})^{1/2}$.

In a laser with Brewster windows, the polarization should be linear (at not too strong a pump), and consequently there are no beats.

The first observations of low-frequency beats in a longitudinal magnetic field were reported by Statz et al.[2] They used a flat He-Ne laser with 1 m distance between mirrors. By passing the laser emission through a linear polarizer at low excitation levels, they observed amplitude modulation of the signal, with a frequency proportional to the magnetic field intensity and to the ratio $\Delta\omega_n/\Delta\omega_D$ (see formula (4.3)). No detailed study was made in [22] of the dependence of the beat frequency on the magnetic field.

Low-frequency beats in a magnetic field were the subject of studies by Culshaw, Kannelaud, and Lopes [6,12,23], and also by Tobias and Wallace [24]. The most interesting data on this question were obtained by Culshaw and Kannelaud [6,25]. In [6] they used a short He-Ne laser ($\lambda = 1.15\ \mu$) with distance 28.3 cm between mirrors. The excitation was with a high-frequency generator. In view of the large separation of the axial modes (530 MHz), such a laser, except when very strongly excited, operated in the single-mode regime. Measures were taken to screen the laser thoroughly against stray magnetic fields and the earth's field. According to the authors' estimate, the residual magnetic field in the laser did not exceed 0.1 Oe. A characteristic plot of the frequency of the low-frequency beats against the intensity of the longitudinal magnetic field, obtained in [6], is shown in Fig. 10. The plot of Fig. 10 corresponds to the case of exact tuning of the resonator ($\omega_n = \omega_0$, $\delta = 0$). As seen from Fig. 10, in this case, at $H < 16$ Oe, the dependence of the beat frequency on the magnetic field is nonmonotonic*. This form of the curve is connected with the nonlinear effects discussed above, and was theoretically explained in [7-9].

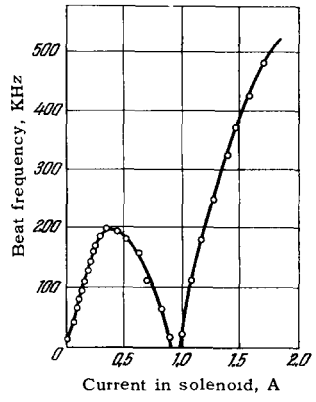

FIG. 10. Dependence of the low-frequency beat frequency on the longitudinal magnetic field intensity for a single-mode He-Ne laser ($\lambda = 1.15\ \mu$) [6]. (Resonator tuned to center of the atomic line.)

The curve of Fig. 10 corresponds to a curve of type 6 or 7 in Fig. 9. Culshaw and Kannelaud did not determine the sign of the beat frequency $\Delta = \omega_1 - \omega_{-1}$, so that to compare Figs. 9 and 10 it is necessary to reflect the initial section of curve 6 or 7 on Fig. 9 about the abscissa axis. The authors indicate that the value of the magnetic field at which the beat frequency vanishes (corresponding to H = 16 Oe in Fig. 10) depends essentially on the pump. No nonmonotonic dependence of the beat frequency on the magnetic field is observed at very low excitation levels (see curves 1—3 on Fig. 9). Thus, the results of a theoretical analysis of the beats between oscillations with RCP and with LCP in a longitudinal magnetic field [7-9,11] are in good qualitative agreement with

*In very weak magnetic fields (on the order of tenths of an Oersted), no beats were observed at all in the experiments of Culshaw and Kannelaud [6]. In the scale of Fig. 8, this small region near H = 0 cannot be discerned. Interesting polarization phenomena have occurred in this region (see Sec. 5).

the data of Culshaw and Kannelaud [6]. The nonlinear dependence of the beat frequency on the magnetic field was observed later by Bolwijn [26] and also by Skolnick et al.[27] Experimental data on the dependence of the beat frequency on the magnetic field at different cavity detunings δ were obtained by Bolwijn [28] and by Culshaw and Kannelaud [25].

The nonmonotonic behavior of the beat frequency near the point $\Omega = \delta$, which results from the theoretical analysis given in [11], has not yet been observed in so far as we know.

In the multimode regime, the picture of the beats in the magnetic field is much more complicated. Owing to the different positions of the modes relative to the center of the atomic line ω_0, the low-frequency splittings differ for the different modes. With increasing pump energy, the number of simultaneously generated modes increases, therefore new components appear in the spectrum of the low-frequency beats. This is illustrated in Fig. 11, which shows the spectrum of the low-frequency beats obtained by Culshaw and Kannelaud [16] at different pump levels. A flat He-Ne laser ($\lambda = 1.15\ \mu$) was placed in a longitudinal magnetic field H = 30 Oe. The resonator length was 125 cm. A detailed interpretation of the spectrum of the low-frequency beats in the multimode regime is quite difficult, since it requires allowance for the mode competition.

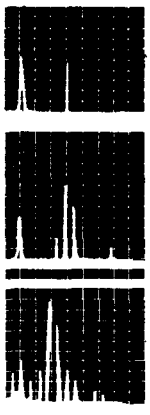

FIG. 11 Spectrum of low-frequency beats in multimode operation of a flat He-Ne laser ($\lambda = 1.15\ \mu$) in a longitudinal magnetic field (H = 31 Oe) [16]. High-frequency pump power a) 150 W, b) 220 W, c) 300 W.

The usual beats between different axial modes [14] in the presence of a magnetic field have interesting singularities, as observed by Paananen, Tang, and Statz [29] They used a flat He-Ne laser of the Javan type, with a distance of 1 m between mirrors (distance between axial modes $\Delta\omega_n/2\pi = 150$ MHz). The pumping was with a high-frequency generator. The low-frequency beats described above were investigated at weak excitation. In the case of sufficiently strong excitation, they observed beats at multiples of 150 MHz, and to observe the beat signal in weak magnetic fields it was necessary to use a polarizer. The reason was that the polarizations of neighboring modes are mutually orthogonal. Similar results were obtained in [16] Paananen et al.[29] observed 150-MHz beats even without an analyzer when the longitudinal magnetic field was increased (H > 13 Oe).

The dependence of the beat signal on the magnetic field, obtained under these conditions in [29], is shown in Fig. 12. The beat signal could be observed without a polarizer because the modes far from the center of the atomic line ω_0 are not split in a sufficiently strong longitudinal magnetic field (the generation condition is satisfied for only one of the circular polarizations). This situation is shown in Fig. 13, from which we see that 150-MHz beats are possible between LCP oscillations (1, 2) and between RCP oscillations (3, 4). With further growth of the magnetic field, the gain for the emission components 2 and 3 becomes lower than the threshold, and these components are attenuated. Then no beats are observed without a polarizer. In Fig. 12 this corresponds to the vanishing of the signal at H = 80 Oe. In even stronger magnetic fields, the laser emission consists of two waves with RCP and with frequencies $\omega_n + \Delta\omega_n$ and $\omega_n + 2\Delta\omega_n$, and also two waves with LCP with frequencies $\omega_n - \Delta\omega_n$ and $\omega_n - 2\Delta\omega_n$. It is seen from Fig. 12 that in this case a beat signal appears again. The dips shown in Fig. 12 (marked by the arrows) in the beat signal occur at magnetic fields such that $2\Omega = \Delta\omega_n, 2\Delta\omega_n, \ldots$ In [29,30] the following explanation is offered for these dips. The authors have shown that even if all four components

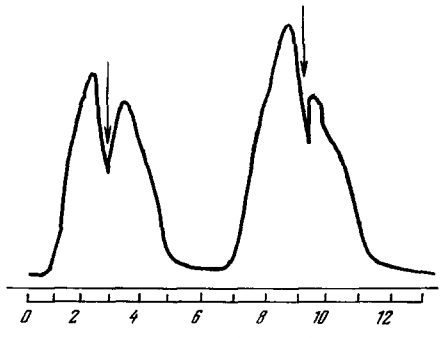

FIG 12. Dependence of the beat signal at 150 MHz (without the use of a linear polarizer) on the longitudinal magnetic field (1 A = 12.8 Oe) [29]

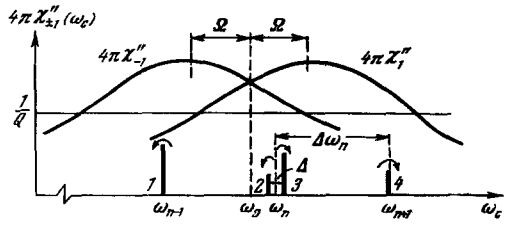

FIG. 13 Schematic representation of the generation-frequency spectrum of a gas laser in a longitudinal magnetic field with excitation sufficient for generation at two axial modes within the limits of each of their Zeeman components.

shown in Fig. 13 are present in the emission, the beat signal can vanish under the following conditions:

$$\theta = (2n+1)\pi, \quad n = 0, 1, 2, \ldots, \tag{4.4}$$

$$I_1 I_2 = I_3 I_4, \tag{4.5}$$

where θ is the phase shift of the 150-MHz beats between the components 1, 2 relative to the beats between components 3, 4. I_k is the intensity of the k-th component. These conditions have a simple meaning. Relation (4.5) signifies that the amplitudes of the beat signals between the components 1, 2 and 3, 4 are equal, and the equality (4.4) corresponds to the fact that these beats are opposite in phase. Condition (4.4), as shown in [29,30], coincides with the condition for the maximum of the total emission intensity, and should always be satisfied. If the modes of the resonator are asymmetrical relative to the transition frequency ω_0, then the second condition (4.5), as seen from Fig. 13, is satisfied only when $2\Omega = \Delta\omega_n, 2\Delta\omega_n, \ldots$. In the case of symmetrical arrangement of the modes relative to the frequency, both conditions are satisfied in all magnetic fields. Then no beats should be observed without a polarizer. It is proposed in [29] to use this effect for exact tuning of the resonator.

An investigation of the phase relations in the multimode regime was carried out also in [31].

5. Polarization Effects

The beats between oscillations with RCP and LCP, discussed in the preceding section should come into play in a flat laser at arbitrarily small longitudinal magnetic fields. However, in the experiments of Culshaw and Kannelaud [6] and Lang [32], with the resonator tuned exactly to the center of the atomic line ($\delta = 0$), these beats were observed only at a magnetic field exceeding certain critical value, of the order of tenths of an Oersted. Culshaw and Kannelaud observed at $H > H_0$ linear polarization whose direction rotated through an angle $\sim 45°$ as the magnetic field increased from 0 to H_0. In the absence of a magnetic field, the laser emission was polarized in a certain direction determined by the weak anisotropy of the mirrors*. So far, when speaking of a flat laser, we had in mind a resonator which is ideally isotropic in a plane perpendicular to its axis. The presence of weak anisotropy denotes that the loss energy for radiation polarized, say, along the x axis is smaller than the loss for radiation polarized along the y axis. Therefore Eqs. (2.2) and (2.12) should be modified by introducing different figures of merit Q_x and Q_y ($Q_x > Q_y$) for oscillations polarized along the x and y axes respectively. The theory of a gas laser in a longitudinal magnetic field in the presence of weak anisotropy of the resonator was presented in [8]. Correct qualitative considerations on this subject were first advanced by Lang [32] (see also [33,34]). We shall attempt below to explain the nature of the arising polarization effects by using simple physical considerations. We confine ourselves here to the case when the pumping is close to threshold and the resonator is exactly tuned to the center of the atomic line ($\delta = 0$).

We assume for simplicity that one resonator mirror (A) is ideally reflecting and isotropic. Let the second mirror (B) have a reflection coefficient R_x for light polarized along the x axis and a reflection coefficient R_y for light polarized along the y axis ($R_x > R_y$). If the anisotropy of mirror B is weak, then the ratio R_y/R_x is close to unity, and we can write

$$\frac{R_y}{R_x} = 1 - \beta, \quad \beta \ll 1. \tag{5.1}$$

The values of Q_x and Q_y are connected with the reflection coefficients R_x and R_y by the relations $R_x = 1 - 2kL/Q_x$ and $R_y = 1 - 2kL/Q_y$. We then get for the value of β (for $R_x \approx 1$ and $R_y \approx 1$)

$$\beta = 2kL\left(\frac{1}{Q_y} - \frac{1}{Q_x}\right). \tag{5.2}$$

When a ray of light of frequency ω_n passes from mirror B to mirror A and back, the plane of polarization in a longitudinal magnetic field is rotated through an angle

$$\Delta\varphi_\Omega = 2 \cdot kL \frac{1}{2}(4\pi\chi'_{-1} - 4\pi\chi'_1), \tag{5.3}$$

where χ'_q is the real part of the polarizability of the gas and is given by formula (2.7). Near threshold we can use the linear approximation (2.8). When the resonator is tuned accurately ($\delta = 0$) and the magnetic field is weak ($\Omega \ll ku$) we get from (2.8) and (5.3)

$$\Delta\varphi_\Omega = 4\pi\alpha \frac{2}{\sqrt{\pi}} \frac{\Omega}{ku} kL.$$

Under the same conditions, the imaginary part of the polarizability at threshold is $\chi''_q = \alpha$. The generation condition requires that

$$4\pi\alpha = \frac{1}{Q_x} \approx \frac{1}{Q_y}\ ^*), \tag{5.4}$$

and therefore we obtain as a final expression for the angle of rotation of the plane of polarization of the magnetic field

$$\Delta\varphi_\Omega = \frac{1}{Q_x} \frac{2}{\sqrt{\pi}} \frac{\Omega}{ku} kL. \tag{5.5}$$

*The correctness of this conclusion was confirmed by the succeeding experiments of Culshaw and Kannelaud [25]. In the absence of a magnetic field the polarization plane was rotated when one of the mirrors was rotated about the laser axis.

*Actually when account is taken of the anisotropy of mirror B, the obtained generation condition is more complicated (see [8]). However, if the reflection coefficients R_x and R_y differ little from each other, then we can use condition (5.4) with good approximation.

We note that in a gas laser this angle is always small. For the existence of a stationary mode in which the laser emission is linearly polarized it is necessary that the Faraday rotation $\Delta\varphi_\Omega$ in the magnetic field be compensated upon reflection by mirror B. Let us calculate the polarization-plane rotation which occurs upon reflection from mirror B. Assume that a light ray whose polarization direction makes an angle φ with the direction of the best reflection (x axis) is incident on the mirror B. If the real amplitude of the electric field in the incident wave is denoted by E, then the components $\tilde{E}_x$ and $\tilde{E}_y$ of the intensity of the electric field in the reflected wave are equal to

$$\tilde{E}_x = \sqrt{R_x}E_x = \sqrt{R_x}E\cos\varphi,$$
$$\tilde{E}_y = \sqrt{R_y}E_y = \sqrt{R_y}E\sin\varphi.$$

The polarization direction is rotated upon reflection through an angle $-\Delta\varphi_R$, with

$$\operatorname{tg}(\varphi - \Delta\varphi_R) = \frac{\tilde{E}_y}{\tilde{E}_x} = \sqrt{\frac{R_y}{R_x}}\operatorname{tg}\varphi. \qquad (5.6)$$

Using (5.1) and expanding the left side of (5.6) in terms of the small quantity $\Delta\varphi_R$, and the right side in terms of the small quantity β, we obtain

$$\operatorname{tg}\varphi - \frac{\Delta\varphi_R}{\cos^2\varphi} = \left(1 - \frac{\beta}{2}\right)\operatorname{tg}\varphi,$$

hence

$$\Delta\varphi_R = \frac{1}{4}\beta\sin 2\varphi. \qquad (5.6')$$

Thus, the greatest rotation of the polarization direction upon reflection occurs when $\varphi = 45°$.

The condition for the existence of a stationary mode with linear polarization of the radiation is $\Delta\varphi_\Omega = \Delta\varphi_R$. From this we obtain with the aid of (5.5), (5.6), and (5.2) the inclination of the plane of polarization of the radiation as a function of the magnetic field:

$$\sin 2\varphi = \frac{\Omega}{\Omega_0}\ ^{*)}, \qquad (5.7)$$

where

$$\Omega_0 = \frac{\sqrt{\pi}}{4}\frac{Q_x - Q_y}{Q_x}ku \qquad (5.8)$$

is the critical value of the Zeeman splitting. When $\Omega > \Omega_0$, formula (5.7) does not hold. In such magnetic fields, the rotation of the polarization plane upon reflection cannot compensate for the Faraday rotation in the magnetic field ($\Delta\varphi_R < \Delta\varphi_\Omega$), and the plane of polarization of the radiation begins to rotate in time. In other words, two oscillations appear, with frequencies that are shifted on both sides of ω_n. As shown by an analysis [8], these oscillations are polarized in right- and left-hand ellipses inclined 45° to the x axis. When $\Omega \gg \Omega_0$, the ellipses turn into circles, and the difference between Q_x and Q_y becomes insignificant. The beat frequency at threshold is given for $\Omega > \Omega_0$ by the formula

$$\Delta = \frac{2}{\sqrt{\pi}}\frac{\omega_n}{Q_x}\frac{\sqrt{\Omega^2 - \Omega_0^2}}{ku}. \qquad (5.9)$$

The results of a qualitative investigation of the mode in which the pump exceeds the threshold value[8] is shown schematically in Fig. 14. The ordinates represent (in units of $\omega_n/2\,(1/Q_y - 1/Q_x)$) the beat frequency which would obtain when $Q_x = Q_y$, and the abscissas represent the Zeeman splitting Ω. Curves 1—7 of Fig. 14, numbered in increasing order of pump energy, correspond to curves 1—7 of Fig. 9. The curves cross the abscissa axis at magnetic fields such that $\Omega \sim \gamma_{10}$. The points of intersection of curves 1—7 with the straight lines ±1 determine approximately the critical field as limits of the regions of linear polarization. The dashed parts of the curves, contained between the horizontal lines ±1, represent approximately plots of the function $\sin 2\varphi(\Omega)$ for different pump values, where φ is the angle of rotation of the polarization direction away from the x axis. The line 1 corresponds to threshold pump. The dashed part of line 1 is described by formula (5.7). The dashed curves do not describe the rotation correctly near the values $\sin 2\varphi = \pm 1$.

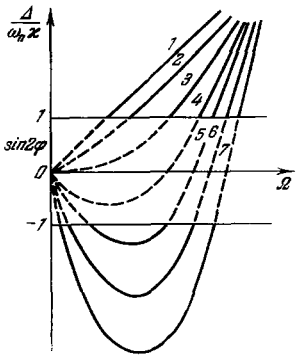

FIG. 14. Schematic dependence of the frequency Δ of low-frequency beats and the angle φ of rotation of the polarization on the longitudinal magnetic field at exact tuning of the resonator [8]. (The pump increases from curve 1 to curve 7.)

The actual beat frequency produced for different values of Q is described by the solid parts of curves 1—7 away from the lines ±1. We see from Fig. 14 that as the pump increases from the threshold value, the critical Zeeman splitting Ω_0 first increases (curves 1—4), and the rotation of the polarization direction slows down. Curve 4 corresponds to a nonmonotonic dependence of the angle of rotation Ω on the magnetic field. The angle φ is initially negative, then vanishes, after which it increases to ~45°. Curves 5—7 correspond to the existence of two regions of linear polarization, separated by a region where beats are observed between two circularly polarized oscillations with different frequencies. For

*Expression (5.7) differs from the result of the rigorous theory [8] by a small term. We note also that if the active medium does not fill the entire space between the mirrors, then L in (5.5) is replaced by the length of the active gas column l. An additional factor L/l then appears in the right side of (5.8), i.e., the critical magnetic field increases.

these curves, the critical splitting Ω_0 decreases with increasing pump energy, the rotation of the polarization direction becomes faster, and the critical magnetic field corresponds to a rotation by $-45°$.

The existence of a second region of linear polarization is connected with the fact that by virtue of the nonlinear effects, at sufficiently strong pumping, the Faraday rotation at $\Omega \sim \gamma_{10}$ decreases and the condition $\Delta\varphi_\Omega = \Delta\varphi_R$ again can be satisfied.

We recall that the foregoing results pertain to the single-mode regime and to the case of exact resonator tuning.

Detailed investigations of the influence of a weak axial magnetic field* on the radiation polarization of a short (L = 28.3 cm) flat He-Ne laser ($\lambda = 1.15\ \mu$) were made by Culshaw and Kannelaud [6,25]. The laser operated in the single-mode regime and was thoroughly screened against the earth's magnetic field and stray fields. Figure 15 shows the dependence of the angle of rotation of the plane of polarization on the magnetic field, obtained in [6]. Curves A and B correspond to 25 and 20 W, respectively, delivered to the discharge. The resonator was tuned in each case for maximum output power. The ratio of the output powers corresponding to curves A and B was 1.45 : 1. The asymmetry of the curves relative to zero current in the solenoid is attributed by the authors to the residual magnetic field. We see that the rotation of the direction of polarization becomes faster with increasing pump. This corresponds to the situation represented by curves 6 and 7 in Fig. 14.

The authors of [6] indicate that thermal detuning of the resonator deteriorates the accuracy of the measurements. To increase the accuracy, a sawtooth magnetic field was used in [6], with frequency 400 cps and amplitude 0.36 Oe. Figure 16 shows oscillograms of the intensity of the output radiation transmitted through the polarizer. The oscillogram 16a corresponds to the polarizer oriented along the direction of polarization in a zero magnetic field (along the x axis), and oscillogram 16c corresponds to polarizer orientation perpendicular to this direction. The oscillogram 16d shows the signal obtained when the polarizer is oriented at 45° to the x axis. Oscillogram 16b, obtained by multiple scanning of the magnetic field, illustrates the thermal detuning of the resonator during the measurement time. The lower part of the oscillograms show the sawtooth current feeding the solenoid. The center of the sawtooth curve corresponds to zero magnetic field. The minimum of the U-shaped curve on oscillogram 16a corresponds to the maximum signal (radiation polarization along the axis in a zero magnetic field). With increasing magnetic field, the rotation of the plane of polarization away from the x axis leads to a decrease in the signal $\sim \cos^2\varphi$. The signal oscillations observed on both sides of the U-shaped curve are due to the appearance of low-frequency beats between oscillations with RCP and LCP at $\Omega > \Omega_0$. The maximum of the inverted U-shaped curve on oscillogram 16c corresponds to the absence of signal.

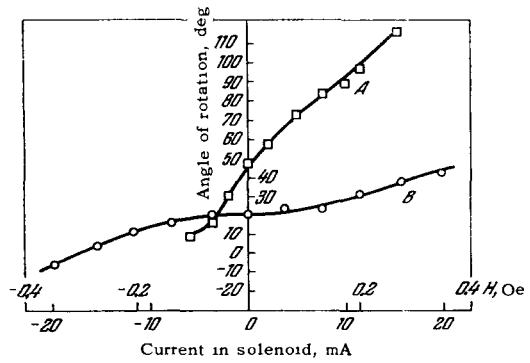

FIG 15. Dependence of the rotation of the direction of polarization of radiation from a flat single-mode laser ($\lambda = 1.15\ \mu$) [16] on the magnetic field. (Curve A corresponds to a pump level 25 W, curve B – 20 W)

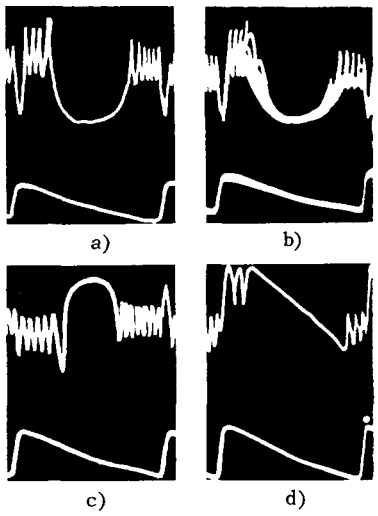

FIG 16. Oscillograms of the laser output radiation intensity for a sawtooth variation of the current in a solenoid (upper parts of the photographs) [6]

The data of Culshaw and Kannelaud [6] make it possible to estimate roughly the difference between the Q_x and Q_y of the resonator employed by them. An estimate shows [8] that this difference was of the order of 0.1%.

In [6] they also observed a second small region of linear polarization at a magnetic field ~15 Oe, where the low-frequency beats vanished (see Figs. 10 and 14). In this region, rotation of the plane of polarization is observed, similar to the rotation of $\Omega < \Omega_0$.

The dependence of the rotation of the plane of polarization of the radiation in a magnetic field on the resonator detuning δ was investigated in [25],

*See [34-36,12] concerning the polarization of radiation from a flat laser in a transverse magnetic field.

where certain interesting data were also obtained on beats occurring near the critical magnetic field. In this paper, Culshaw and Kannelaud point out the role of the anisotropy of the resonator and present a theoretical calculation for the case $j_1 = 1/2$, $j_0 = 1/2$. As noted in Sec. 2, in this exceptional case there is no nonlinear interaction between the RCP and LCP oscillations, and therefore the results of the calculations cannot be used for a quantitative comparison with the experiments made with an He-Ne laser. In particular, this pertains to nonlinear effects (thus, for example, in the case when $j_1 = j_0 = 1/2$ there is no minimum of emission intensity at $\Omega = 0$, $\delta \neq 0$).

As in their earlier paper [6], the authors relate certain effects occurring when the gas laser is placed in a magnetic field with the presence of coherence between the Zeeman sublevels. In particular, they present an analogy between the rotation of the plane of polarization, which they observed, and the Hanle effect in scattering of resonant radiation.

We wish to emphasize in this connection that none of the effects described in Secs. 3—5 is due to coherence between the magnetic sublevels (i.e., to the presence of the nondiagonal elements $f_{mm'}$ and $f_{\mu\mu'}$), although this coherence must be taken into account in detailed quantitative calculations (see Secs. 2 and 3).

6. Use of the Zeeman Effect for Broadband Variation of a Gas Laser Frequency

The possibility of tuning the frequency of a gas laser by using the Zeeman effect was investigated experimentally by Fork and Patel [37]. The splitting of the energy level of the atoms in a magnetic field makes it possible to change over a wide range (on the order of 10 GHz) the frequency at which the gas laser generates. The distances between the centers of the components of the gain for light with RCP and LCP (see Sec. 2) are

$$2\Omega_{m\mu} = 2(m\Omega_1 - \mu\Omega_0) = \frac{2\mu_0 H}{\hbar} g_{m\mu}. \qquad (6.1)$$

where $g_{m\mu} = mg_1 - \mu g_0$ is the effective g-factor, and m and μ are the magnetic quantum numbers of the upper and lower working levels, respectively, satisfying the selection rule

$$m - \mu = 0, \pm 1. \qquad (6.2)$$

The number of Zeeman components into which the gain of the active medium splits in the magnetic field is determined by the number of possible values of $g_{m\mu}$. At sufficiently high gain and high resonator Q, the laser can generate simultaneously at modes lying within each of the components of the gain curve. Both longitudinal and transverse magnetic fields can be used for magnetic tuning of the gas-laser frequency.

With the aid of various anisotropic elements (Brewster windows, polarizers, quarter-wave plates, etc.) it is possible to select oscillations with different frequencies and polarizations.

In the case of a long multimode laser with Brewster windows, and sufficiently high gain (when the generation conditions can be satisfied for the individual Zeeman radiation components, and not only in the region of their appreciable overlap), the laser tuning by means of the magnetic field can be regarded as continuous, since the discrete character of the resonator frequency spectrum can be disregarded when $\Delta\omega_n = \pi c/L \ll \Delta\omega_D$. The possibility of using the Zeeman effect to vary the frequency of a laser is attractive from the point of view of the use of gas lasers for communication and radar purposes, and for the construction of tunable generators and broadband amplifiers [37].

An exact measurement of the Zeeman splitting in strong magnetic fields

$$\Delta\lambda_H = \frac{4\pi c}{\omega_0^2}\Omega_{m\mu} \qquad (6.3)$$

makes it possible to determine the quantity

$$g_{m\mu} = \frac{m}{e}\frac{\omega_0^2}{2\pi}\frac{\Delta\lambda_H}{H} \qquad (6.4)$$

and by the same token obtain information on the real values of the g-factors of the states. Comparison of these data with the theoretical values of the g-factors can serve as a check on the correctness of the chosen scheme of connection between the angular momentum of the working states. The magnitude of the Zeeman splitting $\Delta\lambda_H$ of the emission from a gas laser placed in a strong magnetic field (on the order of 1 kOe) can be measured either with an optical spectrometer of high resolution, or with the aid of a Fabry-Perot interferometer. For example, when $\lambda = 1.15\ \mu$ ($\omega_0/2\pi = 2.6 \times 10^{14}$ Hz), H = 1 kOe and $g_{m\mu} \sim 1$ we get $\Delta\lambda_H \sim 0.1$ Å – a splitting which can be readily measured with the aid a high-resolution spectrometer.

For a laser with He-Xe mixture ($\lambda = 2.0261\ \mu$, transition $5d[3/2]_1^0 - 6p[3/2]_1$, gain ~120% per meter), the Zeeman splitting of the emission line in longitudinal and transverse magnetic fields was measured by Fork and Patel [37]. They used a laser with quartz Brewster windows and mirror separation L = 2 m. The measurements were made with a high-resolution spectrometer (however, owing to the small difference in the values of $g_{m\mu}$, the individual components with RCP or individual components with LCP were, of course, not resolved). Figure 17 shows the experimental plots obtained in that paper for the splitting and for the intensity ratio I^+/I^- (emission components with RCP and LCP) against the intensity of the longitudinal magnetic field (1 A = 166 Oe). As seen from the figure, a linear dependence of the splitting on H is observed in the entire interval of variation of the magnetic field. At H = 2.6 kOe, the maximum splitting amounts to 6 GHz. It should be noted that the width of the Doppler contour for the considered

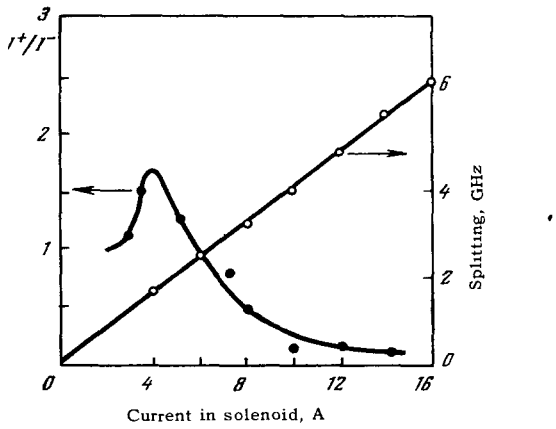

FIG. 17. Dependence of the Zeeman splitting and of the intensity ratio of the emission components with RCP and LCP on the current in the solenoid (1 A = 166 Oe) [37]

transition in Xe does not exceed 200 MHz [38]. Thus, the overlap of the components of the gain coefficients for light with RCP and LCP already vanishes in practice at axial-field intensities H ~ 50 Oe. However, in spite of the presence of Brewster windows, the laser continues to emit at modes with circular polarization also at larger values of H. As in the case of the He-Ne laser with high-Q resonator at wavelength $\lambda = 3.39\ \mu$ [39], this is made possible by the very high value of the gain at the transition with $\lambda = 2.026\ \mu$ in xenon. The variation of I^+/I^- with H, observed in [37], has not yet been explained.

In a transverse magnetic field, the He-Xe laser continued to generate at field intensities reaching 6.8 kOe. The maximum frequency shift amounted to ~8 GHz (~38 $\Delta\omega_D$). As indicated by the author of [37], the emission had circular polarization in a longitudinal field and linear polarization in a transverse field. The experimentally measured splitting turned out to be smaller than the calculated value, this being attributed by the authors to the fact that generation occurred only at the internal components of the "Zeeman set."

In another paper by Fork and Patel [4] dealing with this question, they investigated, besides the He-Xe laser, magnetic tuning of an He-Ne laser ($\lambda = 0.6328$, 1.1526, and 3.3922 μ). A transverse magnetic field with intensity up to 4 kOe was produced by a 102-cm horseshoe electromagnet. A probe operating on the NMR principle was used for the measurement and stabilization of the magnetic field. The laser was a quartz tube with Brewster-angle windows, filled with a mixture of He (p_{He} = 1 mm Hg) and Ne (p_{Ne} = 0.1 mm Hg.). The discharge was excited with a high-frequency generator. The distance between the mirrors of the almost-confocal resonator was 152 cm. The splitting was measured either with a one-meter spectrometer or with a Fabry-Perot interferometer (for the case $\lambda = 0.63\ \mu$). As indicated by the authors of [4], generation occurred not at all the transitions between magnetic sublevels allowed by the selection rule (6.2). The data obtained in [4] on the effective values of the g-factors for the transitions between the magnetic sublevels in neon and the maximum values of the splitting for the He-Ne laser are listed in the table. The values of the g-factors of the upper and lower levels, used for the calculation of $g_{m\mu}$ were taken from Moore's tables [3].

Wavelength, μ	Upper level	Lower level	Values of g_1 and g_0 from [3]	Calculated value of $g_{m\mu}$	Experimental value	Maximum splitting, GHz
0.63	$5s^1\left[\frac{1}{2}\right]_1^0$	$3p^1\left[\frac{3}{2}\right]_2$	1.295 1.301	1.307 1.301 1.295	1.29	14.87
1.15	$4s^1\left[\frac{1}{2}\right]_1^0$	$3p^1\left[\frac{3}{2}\right]_2$	1.33 1.301	2.602 1.33 1.301	1.33	15.37
3.39	$5s^1\left[\frac{1}{2}\right]_1^0$	$4p^1\left[\frac{3}{2}\right]_2$	1.295 1.184	1.295 1.184 1.073	1.09	11.84

The authors of [4] point to a possible influence of the fringing field of the magnet and of competition between modes on the accuracy of the measurements of $g_{m\mu}$.

7. Frequency Stabilization of a Single-mode Gas Laser with the aid of a Magnetic Field

The Zeeman splitting of the intensification (absorption) curve of a gas in a weak axial magnetic field into components with left- and right-circular polarization (LCP and RCP) lead, as is well known, to circular dichroism of the medium.

The anisotropy of the medium, which is connected with the different absorption of the light with RCP and LCP, can be called positive circular dichroism. Conversely, in a medium with population inversion, anisotropy is possible under certain conditions, with respect to the intensification of the light with different circular polarization - negative circular dichroism. The latter phenomenon serves as the basis for a laser frequency stabilization scheme proposed by Tobias et al. [40]. The gain for light with LCP differs from that for light with RCP in all cases when the natural frequency of the resonator ω_n is shifted from the center of the unsplit gain curve ω_0 (see Sec. 3). In the presence of a magnetic field, as shown in Sec. 4, the axial mode splits into a doublet with a frequency gap between the doublet components $\Delta = \Delta_1 - \Delta_{-1}$, which, owing to the frequency pulling effect is approximately smaller by a factor 10^3 than the distance 2Ω between the Zeeman-doublet lines (see Fig. 13). The larger the shift δ of the center of the doublet ω_n relative to the center of the unsplit atomic line ω_0, the greater the difference in the gain, and consequently in the intensity of the emitted light with LCP

and RCP. At sufficiently large values of the shift, when the gain for the light with one of the circular polarizations becomes lower than threshold, a flat laser placed in an axial magnetic field can generate only light with one of the circular polarizations, LCP or RCP. Thus, analyzing the character of the polarization of the emission from a flat single-mode laser placed in an axial magnetic field, we can evaluate the frequency drift of the laser. Tobias et al.[40] analyzed circularly-polarized light with the aid of a $\lambda/4$ plate and a rotating doubly-refracting Roshon prism (Fig. 18). The light with LCP is transformed by $\lambda/4$ plate into light linearly polarized along a definite axis (say, along the x axis), and the light with LCP into light polarized along the y axis. The intensity of the light passing through a Roshon prism rotating with frequency ω_r and striking the photomultiplier is given by

$$I(t) \sim \frac{1}{2} E_{0x}^2 \sin^2 \omega_r t + \frac{1}{2} E_{0y}^2 \cos^2 \omega_r t + \frac{1}{2} E_{0x} E_{0y} \cos \Delta t \sin 2\omega_r t, \quad (7.1)$$

where $\Delta = \omega_1 - \omega_{-1}$ corresponds to the frequency of the low-frequency beats (see Sec. 4), and E_{0X} and E_{0y} are the amplitude values of the field intensity for light passing through a $\lambda/4$ plate with polarization along the x and y axes respectively.

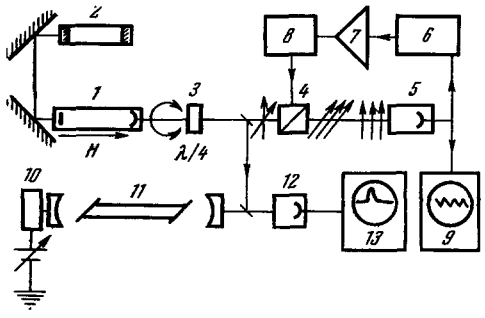

FIG. 18. Block diagram of setup for measurement of frequency detuning of a flat gas laser [40]. 1 – single-mode laser with internal mirror, 2 – Fabry-Perot interferometer, 3 – quarter-wave plate, 4 – rotating Roshon prism, 5,12 – photomultiplier, 6 – tuned amplifier with synchronous detector and reference-signal generator, 7 – power amplifier, 8 – synchronous motor, 9 – oscilloscope, 10 – piezoelectric device for scanning the mirror, 11 – laser with Brewster windows, 13 – spectrum analyzer.

If the detuning $\delta = \omega_n - \omega_0$ of the single-mode laser is large compared with the Zeeman splitting Ω, then the laser will generate light only with one of the circular polarizations. If this light has RCP ($E_{0X} \neq 0$, $E_{0y} = 0$), then the signal at the input of the amplifier is

$$I(t) \sim \frac{1}{4} E_{0r}^2 (1 - \cos 2\omega_r t). \quad (7.2)$$

When the laser frequency drifts to the other side of ω_0, where light with LCP is generated ($E_{0y} \neq 0$, $E_{0X} = 0$), the signal at the amplifier input is

$$I(t) \sim \frac{1}{4} E_{0l}^2 (1 + \cos 2\omega_r t). \quad (7.3)$$

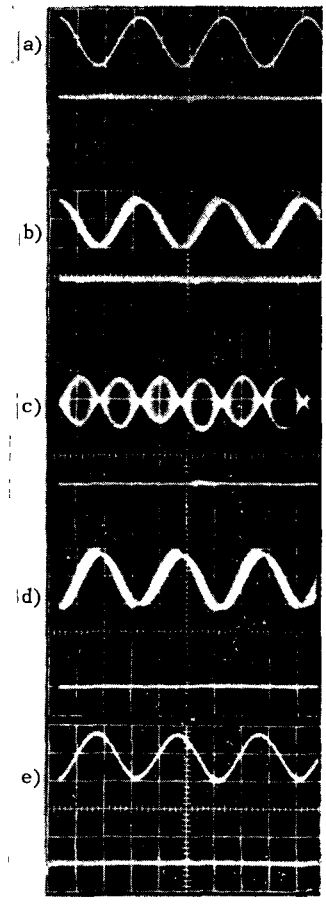

FIG. 19. Oscillograms of input (ac) signal to the amplifier and the output (dc) signal of the synchronous detector at different values and signs of the resonator detuning. The sensitivity for the dc oscillograms is 2 V per large division of the screen.

Thus, in these two cases the ac signals at the input of the amplifier (see Figs. 19a and d) are shifted 180° in phase. The output signal of the amplifier, when detected synchronously with a reference signal of the frequency ω_r as the prism rotation, will be dc (see lower part of the oscillograms in Figs. 19a and e) with polarity that depends on the phase of the sinusoid (7.2) or (7.3) relative to the phase of the reference signal. If the laser generates light with LCP and RCP simultaneously then, as follows from (7.1), the signal at the input of the amplifier will have a form corresponding to the upper oscillogram of Fig. 19b when $E_{0X} \gg E_{0y}$ and to the oscillogram of Fig. 19d when $E_{0y} \gg E_{0X}$. When $E_{0X} = E_{0y}$ (i.e., when $\delta = 0$), the signal will correspond to the oscillogram of Fig. 19c. In the latter case, there will be a zero dc signal at the output of the synchronous detector. Thus, the magnitude and sign of the dc voltage produced by the circuit shown in Fig. 18 are directly connected with the resonator detuning $\delta = \omega_n - \omega_0$. This voltage can be used to correct the laser frequency. A second tunable laser with Brewster-angle windows, shown in Fig. 18, was used by the authors of[40] to measure directly the frequency drift of a flat laser placed in a

magnetic field, using an He-Ne laser (λ = 6328 Å). The intensity of the axial magnetic field in the flat laser was chosen to be 12 Oe.

Unlike the stabilization circuit described above, the operation of the circuit proposed by White et al.[41] to stabilize the frequency of a single-mode He-Ne laser (λ = 6328 Å) with Brewster-angle windows is based on the phenomenon of positive circular dichroism. This stabilization system (Fig. 20) uses an external absorbing cell 3 with gas (Ne^{20}) placed in an axial magnetic field. Since a laser with Brewster-angle windows generates linearly polarized light,

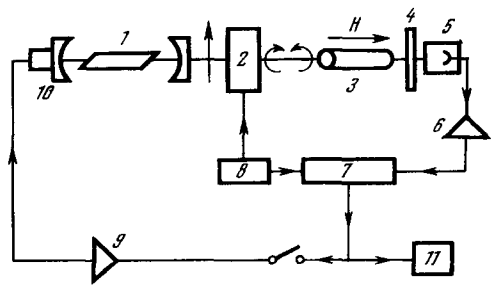

FIG. 20. Block diagram of setup for frequency stabilization of a gas laser with Brewster-angle windows, using an external absorbing cell [41]. 1 – Single-mode laser, 2 – quarter-wave electrooptical switch, 3 – absorbing cell in a magnetic field, 4 – interference filter with 30 Å bandwidth, 5 – photomultiplier, 6 – tuned amplifier, 7 – synchronous detector, 8 – square wave generator with repetition frequency 400 cps, 9 – dc amplifier, 10 – piezoelectric converter, 11 – automatic plotter

this light must be transformed into light with RCP or LCP to effect the frequency discrimination. This was done with a quarter-wave plate. The light of frequency ω_n with RCP, propagating along the magnetic field in a medium without inverse population, will be absorbed only in accordance with the right-hand component of the absorption curve, and light with LCP only in accordance with the left-hand component. If the light frequency ω_n coincides with the center ω_0 of the unsplit absorption curve, then the difference in the absorption of light with different directions of the rotation of the vector E will be equal to zero. The frequency drift causes appearance of a difference in the absorption, which can be used to correct the distance between the mirrors of the laser cavity. The different absorption of the light in the external gas cell can be realized either by periodically reversing the direction of the magnetic field or, leaving the direction of the field in the cell constant, the transition from RCP to LCP can be effected with the aid of a special device - quarter-wave electrooptical switch 2 (Fig. 20). In either case, the laser beam is amplitude-modulated at the switching frequency, the depth of modulation being proportional to the algebraic difference between the absorption coefficients for the RCP and LCP light. By aiming such a beam on photomultiplier 5 connected to a tuned amplifier 6 and a synchronous detector 7, it is possible to obtain the usual discrimination characteristic (the square-wave switching pulses serve in this case as the reference signal). With the feedback loop open, the dc output voltage produced by a change in the laser frequency is fed from the synchronous detector to the automatic plotter 11. When the feedback loop is closed, the error signal is fed through dc amplifier 9 to piezoelectric converter 10, which controls with a high degree of accuracy the length L of the resonator (according to the data of [41], the stability of the emission wavelength was 10^{-5} Å). In the first experiment on magnetic frequency stabilization, White et al.[41] used an absorbing cell with inside diameter 3 mm and length 20 cm. The Ne^{20} pressure in the cell was 5 mm Hg, and the discharge current was 100 mA. It was shown that at small laser-beam absorption in the cell (< 10%) the system had maximum sensitivity at a Zeeman splitting $\sim 0.85\,\Delta\omega_D$ (1.25 GHz). Accordingly, the intensity of the axial field was chosen equal to ~ 350 Oe. The absorption in the cell at 6328 Å was approximately 3 dB/m. The quarter-wave switch was a KDP (KH_2PO_4) crystal.

In concluding this section, we note that an axial magnetic field can be used to increase the sensitivity of a laser gyroscope [32].

II. PLASMA-OPTICAL EFFECTS IN A GAS LASER IN THE PRESENCE OF A MAGNETIC FIELD

In addition to the magnetooptic effects considered in Part I, plasma-optical effects can also arise in a gas-discharge laser placed in a magnetic field. A sufficiently strong magnetic field changes such discharge parameters as the electron density N_e and the average electron energy $\bar{u}_e$ (electron temperature T_e). The form of the function characterizing the electron energy distribution can also change. This in turn should influence the particle pumping condition at the working levels of the gas atoms. The influence of the magnetic field on the pumping depends on the concrete operating conditions and construction of the laser (gas pressure, tube diameter, direction of the magnetic field relative to the laser axis, type of pumping, pump power, etc.). Several methods of pumping are used in a gas-discharge laser. The most frequently used is dc excitation of the discharge (dc pumping) and high-frequency excitation (hf pumping). Pulsed high-frequency pumping (phf pumping) and pumping with the aid of a microwave generator (microwave pumping) are less frequently used*. A special type of microwave pumping is effected under electron cyclotron resonance conditions (ecr pumping). In this review we aim to consider the influence of the

*DC pumping can be realized in either the glow-discharge or arc-discharge mode, hf and microwave pumping can be either continous or pulse-modulated

magnetic field on the emission intensity of a gas-discharge laser will all possible pumping types. The literature contains only information on observation of plasma-optical effects due to the influence of the magnetic field in an He-Ne laser excited in the hf-pumping [39] and ecr-pumping [42] modes. A study was also made of the influence of the magnetic field on the intensity of an argon laser with dc pumping (arc discharge) [43].

8. Influence of Magnetic Field on the Pumping (hf Pumping and dc Pumping)

Since the main excitation mechanism in a gas-discharge laser is electron impact, the population inversion, and consequently the gain of the active medium and the output power of the laser, are functions of the electron temperature T_e and the electron density N_e. For example, as is well known, in an He-Ne laser the gain and the output power are maximal at a certain optimal electron density $N_{e.opt}$ which depends for a given wavelength on the gas pressure, the ratio of the gas-mixture components, and the diameter of the discharge tube [44-46]. Figure 21 shows a plot, obtained by Fotiadi and Fridrikhov [46], of the output power of an He-Ne laser ($\lambda = 0.62\ \mu$) against the electron density N_e*. As seen from the figure, at a mixture pressure close to optimal (pd ~ 3 – 4 Torr-mm), and the laser power reaches a maximum at $N_{e.opt} \sim (4-5) \times 10^{10}$ electron/cm^3. At the same time, as shown by Gordon and Labuda [47],

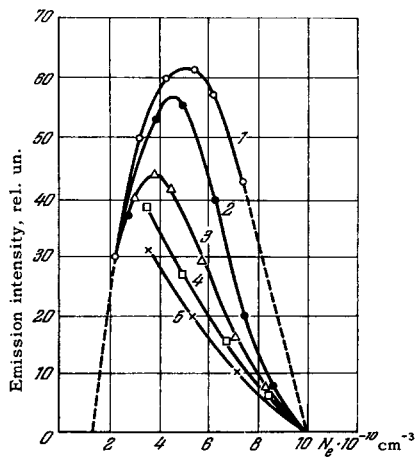

FIG. 21. Intensity of He-Ne laser emission ($\lambda = 0.63\ \mu$) vs. electron density N_e in a gas-discharge plasma [46]. Ratio of the components in the mixture $p_{Ne}/p_{He} = 1/8$. 1 – pd = 3.6 Torr-mm. 2 – pd = 4.8 Torr-mm, 3 – pd = 6 Torr-mm, 4 – pd = 7.2 Torr-mm, 5 – pd = 8.4 Torr-mm.

the electron temperature remains practically constant when pd is constant and the discharge current I_p varies over a wide range. (For example, $T \approx 9 \times 10^4$°K for discharge in helium at pd = 3 Torr-mm and I_d varying from 20 to 100 mA [47].) The number of exciting impacts in a discharge with Maxwellian electron energy distribution* can, in accordance with [5], be written in the form

$$\Delta N_{ik} = N_0 N_e Q_m \left(\frac{kT_e}{eV_k}\right)^{\frac{1}{2}} \exp\left(-\frac{eV_k}{kT_e}\right). \qquad (8.1)$$

where N_0 is the number of atoms in the ground state per unit volume and Q_m is the maximum value of the excitation cross section of the level with excitation potential V_k. In an He-Ne laser, the pumping to the upper working levels (for example, $3s_2$ or $2s_2$) is due to resonant transfer of the energy to the neon atoms in the ground state by the excited atoms of helium (metastable states 2^1s_0 and 2^3s_1). As is well known [52-58], the dependence of the number of excited atoms (say, the He atoms in states 2^1s_0 and 2^3s_1) on the electron density N_e exhibits saturation. This saturation causes the appearance of the maximum on the plot of the He-Ne laser power against the electron density (Fig. 21), inasmuch as the population of the lower working levels (for example, $3p_4$ and $2p_4$) is proportional to N_e [44] or to N_e^2 [59] (for a stepwise excitation mechanism).

The efficiency of a gas-discharge laser, as is well known, is very low (usually << 1%). The pump power delivered to the discharge is partitioned in a definite fashion (see, for example, [60]) among the different frequencies and the thermal losses on the tube walls and in the volume of the gas. The balance of the power consumed by the discharge can be modified by a sufficiently strong longitudinal magnetic field if the latter greatly reduces the coefficient of transverse ambipolar diffusion $D_{a\perp}$ of the plasma electrons towards the discharge-tube walls. As is well known [61], the expression for the coefficient $D_{a\perp}$ is

$$D_{a\perp} = \frac{D_0}{1 + \frac{\omega_e \omega_i}{\nu_{en}\nu_{in}}}, \qquad (8.2)$$

where D_0 is the diffusion coefficient in the absence of the field, ω_e and ω_i are the cyclotron frequencies of the electrons and ions respectively, and ν_{en} and ν_{in} are the frequencies of the collisions between the electrons or ions and the neutral atoms, and depend on the species of the gas atoms and on the pressure (for example, $\nu_{en} \approx 2.4 \times 10^9 p$ and $\nu_{in} = 2.10^7 p$ for He).

A longitudinal magnetic field has a strong influence on the plasma parameters (N_e and T_e) if the following conditions are satisfied: 1) the inequality $\omega_e\omega_i > \nu_{en}\nu_{in}$ must hold, and 2) the Larmor radius of electrons $\bar{\rho}_e = (1/\omega_e)(2kTe/m)^{1/2}$ should be considerably smaller than the diameter d of the discharge tube (more accurately, $\bar{\rho}_e \ll l_\perp$, where $l_\perp$

*The electron density in a laser plasma was measured in [46] by the microwave (resonator) method [48].

*As shown in a number of papers [49-51], rather strong deviation from Maxwellian distribution is observed in the region of the "tail" of this function at not too large discharge currents and gas pressures.

$= N_e/|\nabla_\perp Ne|$ is the characteristic dimension of the inhomogeneous region of the plasma). The second condition is less important than the first, which follows directly from (8.2). The decrease in the radial electron flux under the influence of the magnetic field causes an increase in the electron density N_e at the laser axis. At a fixed discharge current, the growth in N_e produces a drop in the potential gradient E_z in the plasma

$$E_z \sim \frac{I_p}{\lambda_c} \qquad (8.3)$$

This in turn increases the electron temperature T_e.

It should be noted that the increase in the electron density with increasing magnetic field is usually observed only up to a certain critical value $H = H_{cr}$, starting with which the rate of escape of particles from the plasma increases rapidly (see, for example,[61]). At the same time, the potential gradient E_z and the intensity of the plasma noise at microwave frequencies increase. For example, for a discharge in helium with a tube radius 1 cm and gas pressure ~ 1 mm Hg we have $H_{cr} \sim 2000$ Oe[61]. As is well known, the anomalous escape of charged particles from the plasma at $H > H_{cr}$ was explained by Kadomtsev and Nedospasov[62] on the basis of the theory of helical instability.

The influence of the magnetic field on the intensity of the spectral emission of the gas discharge at optical frequencies was studied in detail by Fabrikant and Rokhlin[63-65]. There are also many published papers devoted the influence of homogeneous and inhomogeneous magnetic fields on various electric characteristics of a plasma (N_e, E_z, T_e, $f(u_e)$). At the same time, plasma-optic effects occurring when a gas-discharge laser is placed in a magnetic field have not yet been sufficiently thoroughly studied.

At the gas pressures and tube diameters customarily employed in gas lasers, plasma-optical effects begin to come noticeably into play at longitudinal magnetic field intensities $H \gtrsim 100$ Oe.

Figure 22 shows plots obtained by Ahmed and Kocher[39] of the intensity of an He-Ne laser emission (pd = 3.6 Torr-mm) at 3.9 μ against the intensity of the longitudinal magnetic field. The ratio of the mixture components was 1/5 (p_{Ne} = 0.1 mm Hg, p_{He} = 0.5 mm Hg). Pumping was with a high-frequency generator. A laser with windows perpendicular to the tube axis was used. Plates were placed at the Brewster angles inside the resonator specially in order to ascertain their influence on the dependence of the laser power on the magnetic field. As shown from Fig. 22 at non-optimal pump power (curves 2, 2′ and 3, 3′) the output laser power first increases with increasing intensity of the axial magnetic field* and then, after reaching a maximum (at H ~ 500 Oe), it decreases to very small values (at H ~ 2000 Oe). At optimal pumping (curves 1 and 1′) the axial magnetic field only decreased the output power of the laser. Thus, the axial magnetic field can only slightly exceed the power of the He-Ne laser at 3.39 μ wavelength under the condition that the hf pump is not optimal. With this, the electron density probably increases to an optimal value, but simultaneous decrease of the electron temperature with increasing H causes the maximum emission intensity at H ~ 500 Oe (curves 2, 2′, and 3, 3′) to be less than the corresponding value at H = 0 and at optimal pumping (curve 1). The decrease in laser power with increasing H, up to interruption of the generation at H ~ 2000 Oe, is probably due to deviation of the electron density from optimal (see Fig. 21) and the drop in the electron temperature.

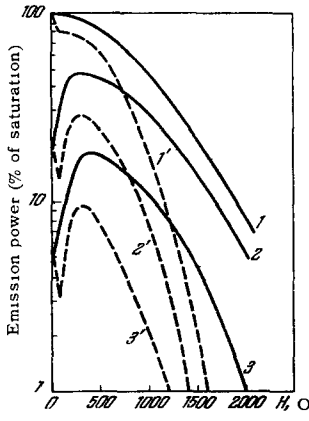

FIG. 22 Intensity of He-Ne laser emission (λ = 3 39 μ) vs. longitudinal magnetic field intensity [39] Ratio of mixture components p_{Ne}/p_{He} = 1 5, pd = 3 6 Torr-mm. Pumping with a high-frequency generator. Curves 1 and 1′ correspond to optimal pumping, curves 2, 2′, 3, and 3′ to non-optimal pumping. Solid curves – windows perpendicular to the axis, curves 1′, 2′, and 3′ – plates installed in the resonator at Brewster angle.

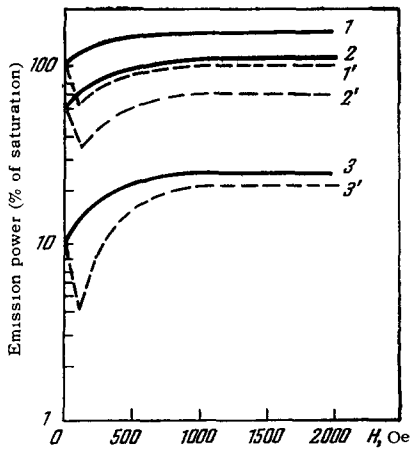

FIG. 23. Intensity of He-Ne laser emission (λ = 3.39 μ) vs transverse magnetic field intensity at different pump powers [39]. Curves 1, 2, and 3 – "flat" laser, curves 1′, 2′, and 3′ – laser with plates at Brewster angles

Figure 23 shows plots of the emission intensity of

*The decrease in power in the case of a laser with Brewster-angle windows (curves 1, 2, and 3) in the region of small values of H(0 < H < 60 Oe) is connected with the selectivity of the windows relative to the polarization of the laser emission. As was shown by Bell and Bloom [20], the intensity of light reflected from the Brewster window in an He-Ne laser at the operating wavelength (λ = 3 39 μ) increases monotonically when H increases from zero to ≈100 Oe.

an He-Ne laser ($\lambda = 3.39\ \mu$), obtained by Ahmed and Kocher [39] in the case of a transverse magnetic field. The small increase in power in case of flat laser at $H < 500$ Oe is apparently connected with the better penetration of the hf-pump waves into the plasma (the discharge is more homogeneous in a transverse field) and with the increase in the electron density.

Of particular interest are investigations of the influence of a magnetic field on the emission power of an argon arc laser (fundamental lines $\lambda = 4880 - 5.45$ Å), in which, unlike an He-Ne laser, no saturation of the emission intensity is observed when the pump power is increased to 10 kW and more [66,67]. However, the efficiency of an argon laser is so far very low ($\sim 0.05\%$), and consequently to obtain powers on the order of 10 W it is necessary to have continuous pump sources with powers of hundreds of kilowatts [67]. The power of an ionized-argon laser increases with increasing discharge current I_d like I_d^n, where $n \gtrsim 2$ [66]. It follows therefore that the mechanism for the excitation of the working levels is stepwise. At optimal conditions of argon-laser operation (pressure $p \sim 0.5$ mm Hg, tube diameter $d \sim 2 - 3$ mm), a noticeable increase in the charged-particle concentration in the plasma is caused by a longitudinal magnetic field with intensity $H \gtrsim 100$ kOe. At a constant discharge current, the increase in the plasma density with increasing H should give rise to an increase in the pump power and in the efficiency of the argon laser.

Golant, Krivosheev, and Privalov [68] investigated the dependence of the charged-particle concentration on the intensity of an axial magnetic field for an arc discharge in argon at $p = 0.5$ mm Hg, and at discharge currents of the order 10—20 A (Fig. 24). The authors of [68] observed an increase in the charged-particle concentration up to $H \approx 2000$ Oe. The maximum concentration was of the order 10^{15} cm^{-3}, corresponding to an argon ionization of several times

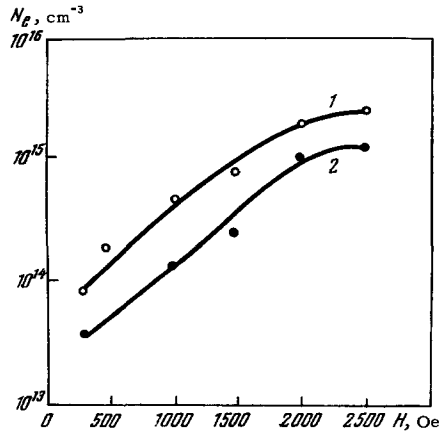

FIG. 24. Concentration N_e of charged particles in an argon plasma vs. intensity of longitudinal magnetic field H [68]. Curve 1 – discharge current I_d – 22 A, curve 2 – $I_d = 10$ A. Argon pressure in the tube $P_{Ar} = 0.5$ Torr.

ten per cent. These data agree well with reports [43] of effective utilization of a magnetic field to increase the output power of an argon laser operating in the dc-pump mode.

9. Electron Cyclotron Resonance in a Gas Discharge Laser (Microwave Pumping)

One of the ways of increasing the efficiency of pumping by electron-atom collisions, as seen from expression (8.1), is to increase the average electron energy u_e. In a laser in which the discharge is excited with a high-frequency generator or a dc source, the average electron energy ($\bar{u}_e = (3/2)kT_e$) is limited, since it is closely connected with other plasma parameters (potential gradient E_z, electron density N_e). It is possible to attempt to overcome this limitation by using microwave heating of the electronic component of the gas discharge with the aid of the method of cyclotron resonance in crossed alternating and constant magnetic fields* [42].

Heating of a gas-discharge plasma with the aid of ecr method was investigated in detail in connection with the problem of producing a high-temperature plasma [72-74]. There are also published papers devoted to a study of the laws governing resonant microwave breakdown in gases [75-83].

As is well known, electron cyclotron resonance can be realized in a plasma when the following conditions are satisfied: 1) The cyclotron frequency $\omega_e = eH/mc$ of the electrons in a constant magnetic field should coincide with the oscillation frequency of the electric microwave pump field, whose **E** vector is perpendicular to H; 2) the frequency ν_{en} of the collisions between the electrons and the gas atoms should be much smaller than the cyclotron frequency; 3) the diameter d of the discharge tube should greatly exceed the average Larmor radius of the electron; 4) the microwave pump field should penetrate into the plasma. For low-intensity microwaves propagating along the magnetic field and not perturbing the plasma, the dielectric constant of the plasma is

$$\varepsilon_{1,2} = 1 - \frac{\omega_p^2}{(\omega \pm \omega_e)\omega}, \qquad (9.1)$$

where $\omega_p = (4\pi N_e e^2/m_e)^{1/2}$ is the plasma frequency. The minus sign in the denominator of (9.1) corresponds to a wave with right circular polarization, in which the direction of the electric field intensity vector rotation coincides with the direction of rotation of the electrons around the magnetic force lines. When a wave of this type penetrates into a plasma, and $\omega = \omega_e$, electron cyclotron resonance takes place, i.e., the electron moving for a long time

*Another way of increasing the power of a gas laser is to use for pumping a monoenergetic electron beam with energy u_e corresponding to the maximum Q_m of the excitation cross section of the given state (the so-called "triode laser" [69] or "diode laser" [70]).

($\nu_{en}^{-1} \gg \omega_e^{-1}$) in the accelerating electric field will draw energy from the microwave field. The average energy $\bar{u}_e$ acquired by the electron between collisions depends in resonant fashion on the ratio ω/ω_e[81]:

$$\bar{u}_e = \frac{e^2E^2}{m_e(\nu_{en}^2 + \omega_m^2)}, \quad (9.2)$$

where

$$\omega_m^2 = \frac{\nu_{en}^2(\omega^2 + \omega_e^2) + (\omega^2 - \omega_e^2)^2}{\nu_{en}^2 - \omega^2 - \omega_e^2},$$

and E is the rms value of the microwave field intensity. Under the resonance conditions $\omega = \omega_e$ and $\nu_{en} \ll \omega$, expression (9.2) simplifies to

$$\bar{u}_e = \frac{e^2E^2}{2m_e\nu_{en}^2}. \quad (9.3)$$

An important feature of the resonant microwave discharge is that a very small amount of power is necessary for its maintenance[81].

Some data on the measurement of the electron temperature under conditions of cyclotron resonance in He-Ne plasma with the aid of double probe method are reported in[42]. The microwave pumping was at a frequency ν = 2.45 GHz ($\omega = 15 \times 10^9$ sec^{-1}) at a gas mixture pressure p_{mix} = 0.6 mm Hg and a component ratio p_{Ne}/p_{He} = 1:5, and at a discharge tube diameter d = 6 mm. The microwave breakdown under these conditions ($\omega/\nu_{en} > 10$) had a typically resonant character. The authors of[42] have observed an increase in the electron temperature T_e, corresponding, according to their calculations, to an increase in the laser power by a factor of 6. They note, however, that their probe measurements call for verification by other methods.

Figure 25 shows a block diagram of the setup used by Ahmed and Kocher[42] to increase the power of the He-Ne laser (λ = 3.39 μ) with the aid of the ecr-pumping method. The pump power source was a magnetron generator 1, operating at 2450 MHz. The microwave energy was fed through a ferrite divider 2 into the waveguide channel. The latter included a directional coupler 3, loop tuning device 4, and a waveguide tee 5 with short-circuited plugs forming a resonant cavity. A laser tube (l = 100 cm, d = 6 mm) filled with a mixture of He and Ne (0.5 mm Hg He and 0.1 mm Hg Ne) was installed in this part of the waveguide channel. A transverse magnetic field H ⊥ E was produced with a horseshoe electromagnet. The laser could be excited either by ordinary high-frequency pumping (ν_{pump} = 60 MHz) or by microwave pumping (ν_{pump} = 2.45 GHz).

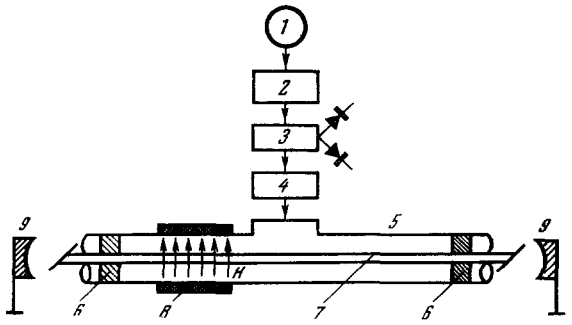

FIG. 25. Block diagram of setup for microwave pumping of a gas laser in the electron cyclotron resonance mode [42]. 1 – Magnetron generator, 2 – ferrite divider, 3 – directional coupler, 4 – loop tuning, 5 – waveguide tee, 6 – short-circuiting stubs, 7 – laser tube, 8 – horseshoe electromagnet, 9 – mirrors.

Figure 26 shows the dependence of the laser power P_g at microwave pumping on the magnetic field intensity H. It is seen that P_g(H) has a resonant character. At H = 879 Oe (the cyclotron field for ν_{pump} = 2.45 GHz) the laser power is approximately doubled. This increase in power was obtained in a magnet of 40 cm length, amounting to 2/5 of the laser length. The authors of[42] indicate that when the entire laser tube is placed in a magnetic field, an increase in the laser power by not less than a factor of 5 can be expected. This agrees with the power-increase estimate which they obtained on the basis of measurements of the electron temperature.

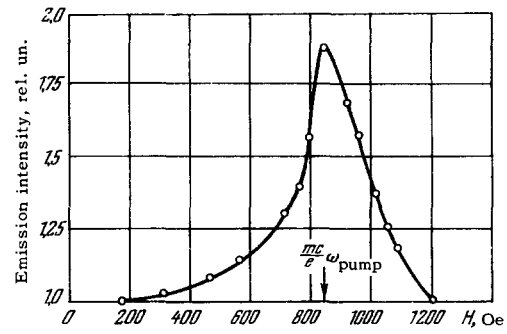

FIG. 26. Intensity of He-Ne laser emission (λ = 3.39 μ) with microwave pumping vs. intensity of transverse magnetic field [42]. The arrow indicates the intensity of the magnetic field corresponding to cyclotron resonance at the pump frequency ω_{pump} (γ_{pump} = 2.45 GHz).

[1] A. Javan, W. R. Bennet, D. R. Herriot, Phys. Rev. Letts. 6, 106 (1961).
[2] W. E. Lamb, Phys. Rev. 134A, 1429 (1964).
[3] C. E. Moore, Atomic Energy Levels, Nat. Bur. Stand., Washington, vol. I, 1949, vol. II, 1952, vol. III (1958).
[4] R. L. Fork, C. K. Patel, Proc. IEEE 52, 208 (1964).
[5] S. É. Frish, Opticheskie spektry atomov (Optical Spectra of Atoms), Fizmatgiz, 1964.
[6] W. Culshaw, J. Kannelaud, Phys. Rev. 136, A1309 (1964).
[7] R. L. Fork, M. Sargent, Phys. Rev. 139, A617 (1965).
[8] M. I. D'yakonov, JETP 49, 1169 (1965), Soviet Phys. JETP 22, 812 (1966).
[9] N. N. Rozanov and A. V. Tulub, DAN SSSR 165, 1280 (1965), Soviet Phys. Doklady 10, 1209 (1966).

[10] C. V. Heer, R. D. Graft, Phys. Rev. 140, A1088 (1965).
[11] M. I. D'yakonov and V. I. Perel', JETP 50, 448 (1966), Soviet Phys. JETP 23, 298 (1966).
[12] M. I. D'yakonov and V. I. Perel', Optika i spektroskopiya 20, 472 (1966).
[13] W. R. Bennet, Phys. Rev. 126, 580 (1962).
[14] W. R. Bennet, Appl. Opt., Suppl. No. 1, 24 (1962).
[15] R. E. Buser, J. Kainz, J. Sullivan, Appl. Opt. 2, 861 (1963).
[16] W. Culshaw, J. Kannelaud, Phys. Rev. 133, A691 (1964).
[17] A. E. Fotiadi and S. A. Fridrikhov, ZhTF 36, 560 (1966), Soviet Phys. Tech. Phys. 11, 416 (1966).
[18] A. Szöke, A. Javan, Phys. Rev. Letts. 10, 521 (1963).
[19] D. K. Terekhin and S. A. Fridrikhov, ZhTF 36, 394 (1966), Soviet Phys. Tech. Phys. 11, 288 (1966).
[20] W. Bell, A. Bloom, Appl. Opt. 3, 413 (1964).
[21] A. Corney, Appl. Opt. 5, 127 (1966).
[22] H. Statz, R. A. Paananen, G. F. Koster, Bull. Am. Phys. Soc. II, 7, 195 (1962); J. Appl. Phys. 33, 2319 (1962).
[23] W. Culshaw, J. Kannelaud, F. Lopes, Phys. Rev. 128, 1747 (1962).
[24] J. Tobias, R. A. Wallace, Phys. Rev. 134, A549 (1964).
[25] W. Culshaw, J. Kannelaud, Phys. Rev. 141, 228, 237 (1966).
[26] P. T. Bolwijn, Appl. Phys. Letts. 6, 203 (1965).
[27] M. L. Skolnick, T. G. Polanyi, J. Tobias, Phys. Letts. 19, 386 (1965).
[28] P. T. Bolwijn, Paper at International Conference on Quantum Electronics, San Juan, Puerto Rico, 1965.
[29] R. Paananen, C. L. Tang, H. Statz, Proc. IEEE 51, 63 (1963).
[30] C. L. Tang, H. Statz, Phys. Rev. 128, 1013 (1962).
[31] H. Lang, G. Bouwhuis, Phys. Letts, 7, 29 (1963).
[32] H. Lang, Philips Res. Repts. 19, 429 (1964).
[33] H. Lang, G. Bouwhuis, Phys. Letts. 9, 237 (1964).
[34] H. Lang, G. Bouwhuis, Phys. Letts. 19, 481 (1965).
[35] M. Dumont, G. Durand, Phys. Letts. 8, 100 (1964).
[36] G. Durand, C. R. Acad. Sci. 258, 510 (1964).
[37] R. L. Fork, C. K. N. Patel, Appl. Phys. Letts. 2, 180 (1963).
[38] C. K. N. Patel, Appl. Phys. Letts. 1, 84 (1962).
[39] S. A. Ahmed, R. Kocher, Proc. IEEE 52, 1356 (1964).
[40] J. Tobias, M. L. Skolnick, R. A. Wallace, T. G. Polanyi, Appl. Phys. Letts. 6, 198 (1965).
[41] A. D. White, E. J. Gordon, E. F. Labuda, Appl. Phys. Letts. 5, 97 (1964).
[42] S. A. Ahmed, R. Kocher, Proc. IEEE 52, 1737 (1964).
[43] Microwaves 3, No. 10 (1964); Electronic News 9, No. 450 (1964).
[44] E. J. Gordon, A. D. White, Appl. Phys. Letts. 3, 199 (1963).
[45] A. D. White, E. J. Gordon, Appl. Phys. Letts, 3, 197 (1963).
[46] A. E. Fotiadi and S. A. Fridrikhov, ZhTF 37, No. 2 (1967), Soviet Phys. Tech. Phys., in press.
[47] E. J. Gordon, E. F. Labuda, J. Appl. Phys. 35, 1647 (1964).
[48] V. E. Golant, ZhTF 30, 1265 (1960), Soviet Phys. Tech. Phys. 5, 1197 (1960).
[49] Yu. M. Kagan and R. I. Ligushchenko, ibid. 31, 445 (1961) and 32, 735 (1962), Soviet Phys. Tech. Phys. 6, 321 (1961) and 7, 535 (1962).
[50] O. P. Bochkova, L. P. Razumovskaya, and S. É. Frish, Optika i spektroskopiya 11, 697 (1961).
[51] N. A. Vorob'yeva et al. ZhTF 34, 2079 (1964) and 33, 571 (1963), Soviet Phys. Tech. Phys. 9, 1598 (1965) and 8, 423 (1963).
[52] S. Levy, Z. Phys. 72, 578 (1931).
[53] K. Schön, Ann. Phys. 28, 649 (1937).
[54] M. Kruse, Z. Phys. 109, 312 (1938).
[55] K. Krebs, Z. Phys. 101, 604 (1936).
[56] R. Ladenburg, UFN 14, 721 (1934).
[57] V. A. Fabrikant and K. Panevkin, DAN SSSR 20, 441 (1938); JETP 9, 1007 (1939).
[58] L. P. Razumovskaya and O. P. Bochkova, Optika i spektroskopiya 9, 271 (1960); 14, 189 (1963); 15, 716 (1963); and 18, 377 (1965).
[59] V. P. Chebotaev, Radiotekhnika i élektronika 10, 377 (1965).
[60] B. N. Klyarfel'd, in: Élektronnye i ionnye pribory (Electronic and Ionic Devices), Trudy, All-union Electrotechnic Institute, No. 41, Gosenergoizdat, 1940.
[61] V. E. Golant, UFN 79, 377 (1963), Soviet Phys. Uspekhi 6, 161 (1963).
[62] B. B. Kadomtsev, A. V. Nedospasov, J. Nucl. Energy C1, 230 (1960).
[63] V. V. Fabrikant and G. N. Rokhlin, DAN SSSR 19, 393 (1938).
[64] G. N. Rokhlin, JETP 9, 801 (1939).
[65] V. A. Fabrikant, Trudy, All-Union Electrotechnic Institute, No. 41, Gosenergoizdat, 1940.
[66] E. J. Gordon, E. F. Labuda, W. B. Bridges, Appl. Phys. Letts. 4, No. 10 (1964).
[67] Electronics 37, No. 32, 14 (1964).
[68] V. E. Golant et al., ZhTF 34, 953 (1964), Soviet Phys. Tech. Phys. 9, 737 (1964).
[69] P. K. Tien, D. MacNair, H. L. Hodges, Phys. Rev. Letts. 12, 30 (1964).
[70] J. M. Hammer, C. P. Wen, Appl. Phys. Letts 7, 198 (1965).
[71] V. G. Bulyginskiĭ et al., Paper 10/242 at the Saltzburg Conference on Plasma Physics, 1961.
[72] M. C. Becker, Suppl. Nucl. Fusion 1, 345 (1962).
[73] W. B. Ard, M. C. Becker, Phys. Rev. Letts. 10, 87 (1963).
[74] A. D. Piliya and V. Ya. Frenkel', ZhTF 34, 1764 and 1752 (1964), Soviet Phys. Tech. Phys. 9, 1364 and 1356 (1965).

[75] A. E. Brown, Phil. Mag. 29, 302 (1940).
[76] B. Lax, W. P. Allis, S. C. Brown, J. Appl. Phys. 21, 1297 (1950).
[77] H. Margenau, Phys. Rev. 73, 297 (1948).
[78] D. J. Rose, S. C. Brown, Phys. Rev. 98, 310 (1955).
[79] A. D. MacDonald, S. C. Brown, Phys. Rev. 76, 1634 (1949).
[80] M. Erisson, J. Appl. Phys. 33, 2429 (1962).
[81] S. Brown, Elementary Processes in Gas-discharge Plasma (Russ. Transl.), Gosatomizdat, 1961.
[82] D. A. Ganichev, S. A. Fridrikhov, B. M. Ashkinadze, and A. B. Solgan, ZhTF 35, 813 (1965), Soviet Phys. Tech. Phys. 10, 633 (1965).
[83] V. E. Golant, M. V. Krivosheev, and I. L. Yachnev, ZhTF 36, 1144 (1966), Soviet Phys. Tech. Phys. 11, 843 (1966).

Translated by J. G. Adashko